In presenting the dissertation as a partial fulfillment of the requirements for an advanced degree from the Georgia Institute of Technology, I agree that the Library of the Institute shall make it available for inspection and circulation in accordance with its regulations governing materials of this type. I agree that permission to copy from, or to publish from, this dissertation may be granted by the professor under whose direction it was written, or, in his absence, by the Dean of the Graduate Division when such copying or publication is solely for scholarly purposes and does not involve potential financial gain. It is understood that any copying from, or publication of, this dissertation which involves potential financial gain will not be allowed without written permission.

_____

_____

7/25/68

A STUDY OF THE ORDERING TRANSFORMATION OF EQUIATOMIC COPPER-PLATINUM

A THESIS

Presented to

The Faculty of the Division of Graduate

Studies and Research

By

Richard John Mitchell

In Partial Fulfillment

of the Requirements for the Degree

Master of Science in Metallurgy

Georgia Institute of Technology

May, 1972

A STUDY OF THE ORDERING TRANSFORMATION

OF EQUIATOMIC COPPER-PLATINUM

Approved:

Chairman

Date approved by Chairman: 5/22/72

ACKNOWLEDGMENTS

The author wishes to thank Dr. B. G. LeFevre for the encouragement and invaluable assistance he afforded throughout the conception, investigation, and writing of this thesis. The author also wishes to thank Drs. E. A. Starke and S. Spooner for their careful reading of the manuscript and their thoughtful advice, and his fellow students for their assistance and moral support. Finally, thanks are due the author's wife, Sue, whose typing and proof reading have been of great aid.

TABLE OF CONTENTS

LIST OF TABLES

LIST OF ILLUSTRATIONS

LIST OF ILLUSTRATIONS (Continued)

SUMMARY

Samples of equiatomic copper-platinum have been quenched from above the ordering temperature into icy brine and annealed isothermally at 300°C, 500°C, and 700°C. Samples annealed for various intervals at these temperatures have been examined by microhardness, optical microscope, electron microscope, and X-ray diffraction techniques. In samples annealed for short times at 300°C and 500°C, a fine-domained mottled structure consisting of all four orientation variants of the ordered cell are seen. Continued annealing develops a coarse-domained grain boundary component which consists of large domains of only one orientation variant. The grain boundary component, which X-ray diffraction shows to have a higher degree of order than the mottled structure, consumes the mottled structure during long anneals. In samples annealed at 700°C, a fine-mottled structure consisting of all four orientation variants is seen initially. During further annealing a twinned structure develops by a coarsening mechanism. In any given area there are two orientation variants - the twins being one and the matrix the other. The individual twins have {100} or {110} twin planes. Both the grain boundary component observed at lower temperatures and the twinned structure observed at 700°C are thoughtto arise in part from the necessity to relieve strains developed in the mottled structure as ordering proceeds. Hardness maxima are correlated with the volume occupied by the mottled structure and the degree of order of the twinned structure.

CHAPTER I

INTRODUCTION

Order-Disorder Transformations

Binary substitutional metallic solid solutions can be of four different types: (a) random solid solutions in which a given component does not prefer a particular kind of atomic neighbor or particular lattice site, (b) short-range ordered solutions in which a given component prefers atomic neighbors of opposite type but does not prefer particular lattice sites, (c) clustered solutions in which a given component prefers atomic neighbors of the same type but does not prefer particular lattice sites, (d) intermetallic compounds in which a given component normally occupies particular lattice sites. Alloys which undergo order-disorder transformations behave as intermetallic compounds at low temperatures, but transform to random or short-ranged ordered solid solutions at some temperature below the melting point (1, 2). This temperature is called the critical temperature and is denoted T_c. At temperatures below T_c, the extent to which particular lattice sites are correctly occupied is given by the long-range lattice parameter, S (3, 4).

Most treatments in the literature consider order-disorder transformations to occur by one of two distinctive mechanisms. One is variously called a first-order, a nucleation and growth, a Gibbsian, or a classical transformation, and is characterized by the formation of ordered nuclei in a disordered matrix. The other mode is referred to as a second order or a homogeneous transformation and is characterized by

a uniform and simultaneous increase in the degree of order throughout the alloy (5). Although these descriptions appear clear-cut and distinguishable, they actually represent extreme cases of a more general mode which is controlled by several contributing factors. As pointed out by Bowles and Malin (6), the first and second-order designations are not appropriate to nonequilibrium transformations.

Most disorder-order transformations occur under nonequilibrium conditions. For structures in which the transformed ordered lattice is similar to the disordered lattice, as in beta-brass, the reaction may occur too quickly to be measureable. The greater the difference between the disordered and ordered lattice, the longer the alloy will take to reach a high degree of order. When the reaction is accompanied by shape or lattice parameter changes, the reaction may take hours or weeks to complete. The strain created by such a transformation would decrease the probability of homogeneous nucleation in favor of nucleation on sites where the strain could most easily be accomodated. Thus, changes in lattice parameter or lattice shape will oppose the ordering transformation, and in their presence the intermediate steps toward order may not occur in a continuous fashion (7).

Above T_c, most ordering alloys have some degree of short-range order. As T_c is approached, the degree of short-range order will usually increase with small areas becoming highly ordered. It is generally accepted that these regions may act as nuclei for the ordering reaction below the critical temperature. At temperatures just below T_c these nuclei will be few in number, but their growth rate into large ordered domains will be rapid. If the changes in lattice shape and lattice

parameter are small, the major impediment to the reaction will be the surface energy between the ordered and disordered regions. If this is small compared with the energy driving the ordering reaction, nucleation can occur homogeneously throughout the grain rather than at grain boundaries or other preferred sites. At temperatures father below T_c more nucleations occur. At sufficiently low temperatures, the nucleations may be so numerous that the reaction may appear to be homogeneous and in fact cannot be distinguished from a homogeneous reaction (5). For this reason it is believed by many (1, 2, 5, 6, 7, 8, 9, 10, 11) that ordering reactions, like most metallurgical reactions, should be treated as nucleation and growth processes. Rudman (12) in his description of ordering kinetics has considered the transformation in terms of three explicit mechanisms: (i) nucleation and growth of ordered domains, (ii) increasing order within the domains, and (iii) domain coalescence after growth and impingement of separate nuclei. Southworth and Ralph (9) have considered in qualitative detail the effects of lattice parameter changes on these mechanisms. They point out that the rate of an ordering transformation and the resulting microstructure will be determined in large measure by the accompanying strains when the misfit between the ordered and disordered lattices is large.

The observed microstructures of some ordered alloys can be explained in terms of a spinodal type mechanism which has been treated by Hillert (13), Cook et al. (14) and by Ling and Starke (15). Hillert uses the zeroth order approximation, which assumes only nearest-neighbor interactions, and allows for variations in the order in one dimension. Cook et al. have extended this analysis to three dimensions for the

early stages of ordering and are in general agreement with Hillert's predictions. Ling and Starke have used a similar approach to derive an expression for the kinetics of ordering which permits the determination of activation energies. These models predict that order develops by the growth of periodic modulations in S and hence, they predict the occurrence of diffuse domain boundaries in the partially ordered state.

All order transformations can be placed in one of two broad categories - - those which do not change crystal system and those which do. Cu_3Au and FeCo are examples of the former, whereas CuAuI and Ni_4Mo are examples of the latter. These have been termed isostructural and neostructural respectively by Guy (16). In the isostructural category the volume changes associated with the ordering process are usually small; consequently, homogeneous nucleation of domains is to be expected. When separate nuclei impinge, they may be out of phase in a translational sense as a result of different sublattice occupation of the two species. The resulting interface is termed an antiphase boundary (APB). In the neostructural case the ordered phase has lower symmetry than the disordered phase; consequently, adjacent domains may be rotated with respect to one another. Such domains have been variously referred to as microtwins (1, 17), transformation twins (7, 8), mosaic structures (7, 8), orientation variants (7, 8), and rotational domains (18). In this discussion, they will be termed orientation variants.

The neostructural alloys are characterized by significant changes in lattice parameter and lattice shape on ordering. The resulting microstructures are somewhat more heterogeneous and complex than those of

isostructural alloys. The most notable effect on properties is a large increase in hardness which appears to be closely related to transformation strains (19). Alloy properties as a function of degree of order have been reviewed by Cahn (20), Stoloff and Davies (19), and Cohen (21); however, investigations into neostructural systems were not numerous at the time. For this reason it is useful to review later observations which have been made of these alloys. This is done in the following section using CuAuI, CoPt, Ni_2V, Ni_3V, and Ni_4Mo as examples.

Observations of Neostructural Alloys

X-ray Measurements

X-ray diffraction observations of alloys which undergo order-hardening may be summarized as follows: (a) at temperatures near the critical temperature, the peaks corresponding to the ordered phase appear immediately and coexist with the disordered peaks and grow in intensity at the expense of the disordered peaks; (b) at temperatures farther below the critical temperature, peaks of the disordered lattice broaden, shift toward the ordered lattice positions, and finally sharpen at the ordered peak positions. The high temperature behavior is consistent with a nucleation and growth transformation mechanism in which the ordered phase can coexist with the disordered phase. Conversely, the low temperature behavior is consistent with a homogeneous transformation mechanism in which the entire structure goes continuously from complete disorder to perfect order. Behavior as in (a) and (b) has been observed in CuAu (1, 6, 22) and Ni_3V (7); only the low temperature effect (b) has been observed in Ni_4Mo (23). Investigations of CoPt by Newkirk *et al*.

(24, 25, 26) have shown just the opposite behavior from (a) and (b). In this case, at low temperatures the ordered peaks were not broadened. They appeared in their final positions, and, at the expense of the disordered peaks, they strengthened. At temperatures closer to T_c, the disordered lines broadened and then sharpened into the positions of the ordered structure. Newkirk et al. have ascribed the high temperature behavior to strain broadening which hides the simultaneous appearance of ordered and disordered peaks. They have claimed that the mechanism is one of nucleation and growth over the entire temperature range. However, work by Southworth and Ralph (9) has shown that at low temperatures the ordered peaks do no initially appear in the ordered positions but rather shift to these positions. They have suggested that the lack of broadening at low temperatures is due to a relief of stresses by the recrystallized grain boundary component observed by Newkirk. Thus the observations of X-ray diffraction in CoPt are consistent with those of CuAu, Ni_3V, and Ni_4Mo.

Quenching

Since many of the neostructural alloys have critical temperatures above 700°C, they are very difficult to quench to disorder. Evidence of order is found in quenched samples of Ni_4Mo (2, 27), Ni_2V (8), and Ni_3V (7).

Mottled Structure

When observed in the transmission electron microscope, (TEM) neostructural alloys sometimes exhibit a fine scale straited or mottled structure.* Although TEM studies have not revealed details of the

*Mottling is a structure consisting of small domains no more than 300 Å in diameter. In the electron microscope they appear as small bright spots on a dark background - hence they appear "mottled".

mottled structure, selected area electron diffraction has shown that such areas contain all possible orientation variants of a given alloy. Mottling is most commonly observed in neostructural alloys after annealing quenched samples in temperature ranges more than 150°C below the alloy's T_c. It is reported in Ni_4Mo below 700°C (2, 27), in CuAu below 350°C (1, 17, 28), in Ni_3V below 600°C (7), and in Ni_2V below 800°C (8). At temperatures closer to T_c, all these alloys develop coarser structures, and mottling is not seen except in the case of very short annealing times. At very short annealing times, the mottled structure which is observed is most likely that which develops during the quench. This is consistent with Syutkin's suggestion (28) that quenching neostructural alloys results in many nucleation sites for ordering. Tanner has shown that Ni_2V (8) does not show mottling at short annealing times near T_c if the sample is quenched to the annealing temperature from above T_c, thereby avoiding low temperature rapid nucleation during the quench.

Tanner (7) has shown that the contrast arising from the mottled structures in the TEM is like that arising from elastic coherency strains. Such contrast can arise from two or more differently oriented structures related by coherent interfaces. In the neostructural alloys the interfaces may be either between the disordered phase and one of the orientation variants or between two different orientation variants. The resulting strain contrast sometimes forms striations in the mottling. These striations are always in the same direction in CuAu and have been used by Hirabayashi and Weissman (17) to index the habit plane of the mottled orientation variants. Additionally, Tanner (7) has used these

straitions to index the habit planes of mottled orientation variants in Ni_3V.

Twinning

Neostructural alloys twin during the ordering transformation. The twin planes separate different orientation variants. The result is a mismatch of reciprocal lattice vectors across the twin boundary which in the electron microscope shows up as δ-fringe contrast (29). The δ-fringe contrast has been observed in Ni_3V (7), Ni_2V (8), and Ni_4Mo (2, 27). The twins may be fine, so that they are observed only in the electron microscope; or they may be coarse, so that they are observed at low powers in the optical microscope. In the range of temperatures more than 150°C below T_c, after long annealing times, the mottled structure is sometimes replaced by a Widmanstatten pattern of fine twins. It has been seen in the electron microscope that after longer anneals these twins coarsen. At temperatures not more than 150°C below T_c, short annealing times produce structures similar to those observed after the longer anneals in the low temperature ranges. Slightly longer anneals in the high temperature range produce coarse twins which can be observed in the optical microscope. These twins, because of more difficult nucleation near T_c, occur preferentially at free surfaces, grain boundaries, and other twins (6).

In tetragonal ordered alloys the twin plane must be a plane that does not contain the tetragonal c-axis. Since these alloys are tetragonally distorted during ordering, the (110) plane of the ordered lattice is the twin plane. Hirabayashi and Weissman (17) have found that in CuAu, (110) twin planes separate orientation variants whose c-axes

alternate XYXYXY... This sequence of orientation variants minimizes the strain which results from the tetragonality of the orientation variants of CuAu. Similar alternating sequences of orientation variants are observed by Tanner in Ni_3V (7) and by Bowles and Malin in CoPt (6).

The development of the twins in neostructural alloys is a central problem in the understanding of how these alloys order. Several investigators have suggested that the strains which develop during the transformation cause the ordered variant to shear. Ashby and Tanner (30) suggest this for Ni_3V just below T_c but add that the twin is only nucleated by shear after which it grows by diffusional addition at its interface. Prior to Ashby and Tanner, Hansson and Barnes (31) had proposed a model for shear twinning in CuAu. Hirabayashi and Weissman (17) attribute all the twinning they observe in CuAu to mechanical deformation which arises from the transformation strains, while Arunachalum and Cahn (1) suggest that only the "macrotwinning" observed by Hirabayashi and Weissman is due to mechanical deformation. Arunachalum and Cahn suggest that the "microtwinning" observed by Hirabayashi and Weissman is due to "accidents in growth" rather than mechanical deformation. This growth mechanism is an alternative to the mechanism of twinning by shear. In growth twinning the twins develop from the impingement of orientation variants. Arunachalum and Cahn note that the only difference between a growth twin and a shear twin is that the composition plane of the shear twin would always be the twinning plane [in these alloys, (110)], while the composition plane of the growth twin could also be the twinning plane since this plane minimizes the distortion between two orientation variants, and the boundary of intersection

between them could adjust to be along this lower energy plane. Tanner (7) for Ni_3V and Syutkin et al. (28, 32, 33) for CuAu have also proposed growth twinning mechanisms. Unfortunately, each of these mechanisms is too specific to be applied to general neostructural alloys. However, aspects of each can be applied to CuPt and hence will be further covered in the Discussion of Results.

Both growth twinning and shear twinning as discussed here are the result of the ordering transformation. A third kind of twinning may develope from mechanical deformation not introduced by the ordering transformation. Although early work (19) on long range ordered alloys suggested that they would not exhibit deformation twinning, such twinning has been observed in neostructural CuAu at room temperature by Pashley et al. (34). To date, CuAu is the only alloy in which deformation twinning has been proven conclusively.

Grain Boundary Components

Some neostructural ordered alloys appear to develop recrystallized grains around the initial grain boundaries. The grain boundaries of other neostructural ordered alloys appear to have migrated to new positions, leaving in their wake highly ordered material of one orientation variant. Grain boundary migration and grain boundary recrystallization have been observed only in annealing temperature ranges more than 150°C below T_c.

The recrystallized "new grains" at the grain boundary were first observed by Newkirk et al. in CoPt (24). They have subsequently been observed by Arunachalum and Cahn in CuAu (1) after long anneals at temperatures at more than 150° C below T_c. Newkirk et al. note that the

recrystallized grains appear more highly ordered than the rest of the alloy and suggest that preferential ordering ocfurs at grain boundary sites resulting in high lattice strains which in turn induces local recrystallization. In addition, Newkirk et al. have observed recrystallized grains at surfaces in CoPt, suggesting that the recrystallization occurs preferentially at free surfaces as well as at grain boundaries.

Arunachalam and Cahn have also observed grain boundary migration in CuAu (1) after short anneals at temperatures more than 150°C below T_c. In the electron microscope the area around the grain boundary appears as ordered material of a single orientation variant separated from mottled material with the same crystalline orientation by a coherent boundary and separated from mottled material with a different crystalline orientation by an incoherent boundary, (i.e. the grain boundary). Arunachalam and Cahn attribute this observation to "strain-induced boundary migration." Cahn (35) describes this as the result of two adjacent grains being in different states of strain. The strain is removed if the grain which is less strained grows at the expense of the more strained grain. As the boundary moves, the material behind it is added to the new grain in a state of perfect order. Similar observations to these in CuAu have been made in Ni_2V (8) and Ni_4Mo (2, 27). In Ni_2V the grain boundary component was observed to sweep through the mottled material, thus completing the ordering transformation.

Intergranular Cracking

Intergranular cracking has been reported in two neostructural alloys, Ni_4Mo (2, 27) and CuAu (1, 28, 32). Cracking is never observed at temperatures where grain boundary components develop. At temperatures

near T_c, Syutkin et al. (28, 32) confirm cracking in CuAu but note that cracking occurs only in specimens which have been disordered, quenched to room temperature, and then raised to the annealing temperature. If the specimen is quenched to the annealing temperature from above T_c, no cracks develop. Syutkin et al. further note that cracking is more prevalent in large-grained specimens than in fine-grained specimens.

Hardness Measurements

As neostructural alloys order, their hardness is greatly affected. At anneals more than 150°C below T_c, the typical behavior is a rapid increase in hardness from the as-quenched state, followed by a slow increase in hardness as annealing continues, and then a decline in hardness as the ordering is completed. This general behavior is observed at low temperatures in CoPt (24), CuAu (1), and Ni_4Mo (2). For samples annealed within 150°C of T_c, the typical behavior is again a rapid increase in hardness from the as-quenched hardness. However, a peak of hardness is reached in less than ten minutes of annealing and a rapid decrease in hardness begins and continues until it is at or below the as-quenched hardness. Thereafter, the hardness levels off, decreasing slowly with time. This sequence is observed in CoPt (24), CuAu (1), and Ni_3V (7). Both the high and low temperature hardnesses can be well correlated with the microstructure of the alloy. In neostructural alloys mottled structures correspond to high hardness, while twinned structures correspond to low hardness.

Hardness values are a function of yield strength and work hardening rate. The effect of order upon these in isostructural alloys has been reviewed by Stoloff and Davies (19), Cahn (20), and Cohen (21).

In general, the mechanism suggested in these papers as giving rise to hardening do not apply to neostructural alloys. The only suggestion unique to neostructural alloys is by Cahn (1) who points to a work hardening mechanism first suggested by Fleischer (36). As a result of the change in lattice parameter which exists at interfaces of adjacent orientation variants or at interfaces separating disordered material from ordered nuclei, a sessile interface dislocation will be left when an edge dislocation passes across the interface. Subsequent dislocations on the same slip plane will be resisted by the first, and each new dislocation will leave another interface dislocation, making movement of dislocations on the slip plane more and more difficult.

Ordering in CuPt

One of the least studied of the neostructural ordered alloys is 50 atomic percent CuPt (37, 38). Equiatomic CuPt orders below 812°C, producing a rhombohedral structure in which alternate copper and platinum layers occupy (111) planes. Above 812°C the disordered lattice is face center cubic. Below 812°C there is a contraction in the direction normal to the ordered (111) planes. The resulting ordered lattice is rhombohedral with 32 atoms in the unit cell. The lattice parameter (7.58 Å) is twice that of the disordered face center cubic and the rhombohedral angles is approximately 91°. The crystal lattice changes from cubic to rhombohedral upon ordering, hence CuPt is neostructural. The ordering can occur on any of the four (111) type planes, and upon impinging domains of two such ordered variants have their axes of contraction rotated with respect to one another. The unit cell of CuPt is unique in two respects. First, its ordered superlattice is the only known configuration of the

Li_1 type. Second, it is the only ordering system in which the atoms have the same number of unlike first nearest neighbors in the ordered state as in the ordered state as in the disordered state.

The structure of equiatomic CuPt was first determined by Johansson and Linde (39) using Debye-Scherrer patterns and electrical resistance measurements. They have shown that superlattice spots appear halfway between odd-indexed face center cubic lattice reflections. These fundamental reflections are slightly rotated from cubic positions due to the rhombohedral transformation. (The indexing of diffraction patterns for ordered CuPt is discussed in Appendix I.) Electrical resistance measurements have been made by Kurnakow and Nemilow (40). Lattice spacing and rhombohedral angle as functions of composition for compositions around 50 atomic percent have been calculated from Debye-Scherrer patterns by Linde in samples which were quenched after anneals at 300°C and 720°C (41). The variation in electrical resistance with temperature and composition and the variation of as-quenched disordered lattice parameters with composition have been measured by Schneider and Esch (42).

Later Debye-Scherrer and diffractometer investigations by Walker (43) have generally confirmed the difference which Linde found in rhombohedral angle measured at 300°C from that measured at 720°C. In addition, Waler calculated the long-range order parameter as a function of annealing temperature and showed that the change in the rhombohedral angle with order is a function of the long-range order parameter. He found that cold work in CuPt will destroy the superlattice peaks and eliminate splitting of fundamental x-ray diffractometer peaks. He also found diffuse superlattice intensities in samples quenched from above

T_c. These intensities were spread over the (111) and (113) superlattice positions*. In order to confirm that this was short-range order which existed above T_c, Walker has conducted x-ray diffractometer investigations of CuPt at 890°C. Although they are more spread out than in the quenched sample, diffuse peaks are still present at this temperature in the (111) and (113) superlattice positions. From these peaks, Walker has calculated the short-range order distribution function and has shown that above T_c copper and platinum partially segregate to alternate (111) planes over a distance of a few lattice parameters.

All available evidence indicates that the ordering transformation in CuPt is first-order. Assayag and Dode (44) have employed oxygen at equilibrium with alloys around the composition of equiatomic CuPt to show that it is a first-order transformation. They have concluded that in off-stoichiometric compositions the ordered phase coexists in equilibrium with the disordered phase. Recent work by Irani and Cahn (11) using x-ray diffraction showed that peaks corresponding to the disordered alloy coexist with ordered peaks in a stoichiometric alloy annealed for three minutes at 765°C. The disordered peaks disappeared after longer anneals. In off-stoichiometric compositions the disordered peaks persisted even after long anneals. By comparing lattice parameter measurements derived from the disordered peak positions with the lattice parameter measurements made by Schneider and Esch as a function of composition in the disordered alloy, Irani and Cahn determined the composition

*The indices used in this paper refer to the 32-atom ordered face center cubic unit cell unless otherwise specified.

of the disordered phase for several temperatures. With this they plotted several points on the "disordus" curve and showed their results to be in agreement with the equilibrium phase diagram of Assayag and Dode. Irani and Cahn also reported (45) a thermal polishing technique with which they observed a grain boundary component similar to that reported in CoPt (24) and CuAu (1).

The fact that the ordered CuPt lattice has the same number of unlike first-nearest neighbors as the disordered lattice has generated much of the research on the alloy. Usually, ordering reactions are considered to result from first-nearest neighbor preference for unlike atoms; but as stated previously, the number of unlike first-nearest neighbors is unchanged in going from ordered to disordered CuPt. Slater (46) has proposed that the Brillouin zone is split by the double periodicity of the lattice. The lowering of the half-period lowers the electron energy if the zone is half-filled with electrons. This lowering of the Fermi energy is suggested as the driving force for ordering. Confirmation of this possibility is found in calculations by Nicholas (47) and electronic specific heat measurements by Roessler and Rayne (48). The latter point out a possible magnetic transition in CuPt.

Reports of work on the mechanical properties of CuPt are scarce. Nowack (49) measured the hardness as a function of isothermal annealing time for CuPt alloys at 500°C and 700°C. At 500°C, the Brinell hardness increases from 130 to 260 in under an hour and levels off at 260 after one hour. At 700°C, the hardness peaks at a Brinell hardness of 200 in under 15 minutes and falls rapidly to below the as-quenched hardness of 130 where it continues to decline.

Few microstructure studies of equiatomic CuPt can be found. Thin foil transmission electron microscopy has been performed by Corke and Amelinckx(50). After rolling to 0.1 millimeter, CuPt samples were heat treated for six days at 760°C or were slow-cooled from above T_c and were polished by using a modification of a polish developed by Ahlers and Balluffi (51). In the foils thus obtained, Corke and Amelinckx observed δ-fringe contrast and antiphase boundaries with a displacement vector (in the superlattice) of a/4[110]. Symmetrical and asymmetrical fringe contrast was accompanied by splitting of fundamental spots in the selected area diffraction patterns of the areas of fringe contrast. These effects were attributed to coherent twins on (100) or (110) twin planes. These twin planes separate two orientation variants whose directions of contraction are rotated with respect to one another. Corke and Amelinckx have also predicted that single dislocations have to split when crossing such a twin boundary. This sould occur because slip in the (111) layered planes can occur by normal dislocations while slip in any other {111} type plane must occur by superdislocations. Since the nature of a {111} type plane changes when crossing a coherent twin boundary, slip by normal dislocations must change to slip by superdislocations.

In addition to the electron microscopy, Brooks (52) imaged CuPt in the field-ion microscope. Using pure Helium with small additions of Neon as imaging gases at liquid nitrogen temperatures, he showed that an image can be obtained which is made up of one of the atomic species. Although Brooks's study concentrates on imaging CuPt in the field-ion microscope, he also observed that after ordering for 5½ hours at 690°C

there is a diffuse order-disorder interface.

At the time of this writing, no study, other than Nowack's hardness measurements, has been made of the kinetics of the transformation in CuPt. The object of the present investigation is to begin such a study by determining the microstructures and hardness of equiatomic CuPt at various ordering temperatures and times. Three principle methods of study are used; hardness measurements, optical metallography, and transmission electron microscopy of samples taken from the bulk. In addition, x-ray diffraction data has been used to supplement the results obtained from these.

CHAPTER II

EXPERIMENTAL METHODS

Preparation of Samples

Melting

The equiatomic CuPt alloy was obtained in button form from Engelhard Industries. They reported that the platinum was 99.95 percent pure and the copper was 99.99 percent pure. They had melted the alloy, using a tungsten electrode in a vacuum arc-melting unit, which was back-filled with argon. The as-received button was remelted into a rod shape using a vacuum arc-melting unit which again was back-filled with argon. The melt was repeated several times, in order to obtain as homogeneous a composition as possible.

Homogenization

After melting, there was a rough surface layer on the rod which was removed mechanically. The sample was degreased ultrasonically and encapsulated in quartz tubing at a pressure of 10^{-5} millimeters of Mercury. The sample was then homogenized for 48 hours at 1200°C in a Lindberg Hevi-Duty furnace (Type 51939). After the homogenization, the sample was quenched in ice water.

Quenching

The quench after homogenization was not rapid enough to prevent the sample from ordering. The quench was improved by reheating the sample and quenching it from 1000°C into icy brine. To achieve as fast a quench as possible, it was desirable to be able to drop the sample

from the hot zone of the furnace directly into the ice brine. Also it was important that the sample did not oxidize.

A resistance furnace was fitted with a vycor tube which could be evacuated to a pressure less than five microns of mercury. The sample was lowered into the hot zone of the furnace when the desired temperature was reached and was quenched by releasing it from its holder and allowing it to drop out of the tube into a bath of icy brine. During the introduction of the sample to the hot zone and during the quench, helium was passed through the tube to prevent oxidation. During the anneal the annealing the vycor tube was evacuated. Agitation of the icy brine helped to give a better quench. Nevertheless, CuPt was never quenched into the disordered state by this procedure.

Rolling and Swaging

Rolling of the CuPt ingot was attempted in order to make sheets from which foils could be made for TEM studies. After small reductions the samples were annealed one hour at 1000°C and with ice brine. Cracking intervened before sufficient reduction had been obtained. More success was achieved in alternately cold swaging and annealing the alloy as above. Although gtreater reduction was obtained by the latter procedure than by cold rolling, cracks also developed in the swaged alloy. Attempts to hot roll a CuPt alloy from another melt also resulted in cracking. The extreme work hardening behavior and brittle cracking that was observed in both cold and hot working may be the result of not being able to quench the sample into the disordered state.

Cutting

The rod obtained by swaging was cut into transverse sections.

which were recrystallized by annealing for one hour at 1000°C and were quenched. Subsequent slices were cut from these pieces and heat treated as desired. To avoid deforming the sample these cuts were made with an electrical spark cutting machine using a wire cutting tool with slow cutting rates.

Heat Treatments

The ordering heat treatments were performed in the vertical furnace previously described. As noted, the samples were introduced into the hot zone after it had reached the desired temperature, thus keeping the heating time minimum. All samples were initially in the as-quenched condition. The quenched alloys were annealed at times ranging from five minutes to 104 hours at 300°C, 500°C, and 700°C. The times of the anneals correspond to the time elapsed between introduction of the sample into the hot zone of the furnace and quenching into ice-brine. No visible contamination resulted from the ordering anneals.

Preparation for Optical Microscopy and Hardness Measurements

Optical microscopy and microhardness measurements were made on the same pieces. After each increment of the desired heat treatment had been completed the samples were mounted in "Quickmount", ground through 600 grit silicon carbide papers, and polished through 0.3 micron alumina. The samples were electrochemically etched by a modification of the polishing technique of Corke and Amelinckx (50). This polish worked best when operated at a current between 0.8 and one ampere.

Preparation for Transmission Electron Microscopy

The alloy CuPt is particularly difficult to electropolish for TEM studies because of its relative opaqueness to electrons and its

chemical inertness. Attempts to electropolish CuPt by the method of Corke and Amelinckx (50) proved unsuccessful. Although polished areas were obtained, usable thin areas were very scarce because of preferential attack at grain boundaries. It was found, moreover, that the behavior of the electropolish depended greatly on how the CuPt alloy had been heat treated.

Attempts to dimple CuPt by the technique of Dubose and Stiegler (54) were largely unsuccessful. A variety of electrolytes were tried at both a.c. and d.c. voltages but in all cases they either produced a black deposit (51), showed a marked tendency for grain boundary attack, or did not polish at all.

The technique finally adopted made use of a sample holder devised by Dewey and Lewis (55) in combination with the electropolishing setup described by Dubose and Stiegler (54). Discs of CuPt 2.3 mm. in diameter were spark-cut and hand ground on 600 grit silicon carbide paper to a thickness under 0.005". The samples were then electropolished in an electrolyte of 0.1 Normal sodium hydroxide at room temperature, 70 volts and 60 cycles a.c. The appearance of a hole was detected by use of a light source-photo cell-relay arrangement. Although this procedure did not completely remove the black film or the grain boundary attack the problems were not as severe and usable foils were obtained.

Experimental Measurements

Hardness Measurement

After each increment of annealing time at each of the three ordering temperatures, hardness measurements were made. The Tukon microhardness tester was used with a Knoop indenter and a 500 gram load.

Averages were obtained for indentations at twelve or more positions across the diameter of a sample cross section. The position from which a particular hardness value was taken was recorded on maps of the samples. Notes were made of the hardness of particular features in the CuPt microstructure.

Optical Metallography

Photomicrographs were taken of samples after each increment of heat treatment, usually before hardness tests were made. Grain size was measured and features of the microstructure were noted.

Transmission Electron Microscopy

CuPt foils were examined with a Siemens Elmiskop 1A electron microscope operated at 100 kV. The microscope was equipped with a Swann double tilting stage and electromagnetic beam tilt for obtaining precision dark-field images. Use of the electron microscope to study thin crystalline specimens has been described by Hirsch et al. (53) and recently by Murr (56). The habit planes of planar features in the electron micrographs were identified by standard trace analysis procedures. Indexing of selected area diffraction patterns was aided by the construction of a reciprocal lattice model of ordered CuPt (see Appendix I).

CHAPTER III

RESULTS

Optical Metallography

The microstructure of as-quenched CuPt is shown in Figure 1a. Large grains with a large number of annealing twins characteristic of face-center cubic systems are shown. Except for small recsytallized grains around intergranular cracks which were produced during swaging, the grain size is uniform across the specimen diameter. It should be noted that the grain boundaries are clear and undistorted.

The microstructures of samples ordered at 300°C and 500°C are almost the same. The first effect of ordering at these temperatures is to produce a thickening of the grain boundaries. Shortly thereafter, a polished surface develops a definite topography. Faint rills and striations appear in the microstructure when the sample is viewed by oblique illumination as in Figure 1b. Similar features appear in samples which were poorly quenched. Figure 2a shows the structure typical of alloys which were ordered over 80 hours at either 300°C or 500°C. The most notable feature of the microstructure is the appearance of grain boundary and surface components which look to be of similar structure. Figure 2b shows a portion of the surface component extending into the center of the sample along a grain boundary. The internal structure of the surface and grain boundary components is somewhat ambiguous. Fine "recrystallized" grains seem to make up this component; however, this may be the result of etching associated with coarse

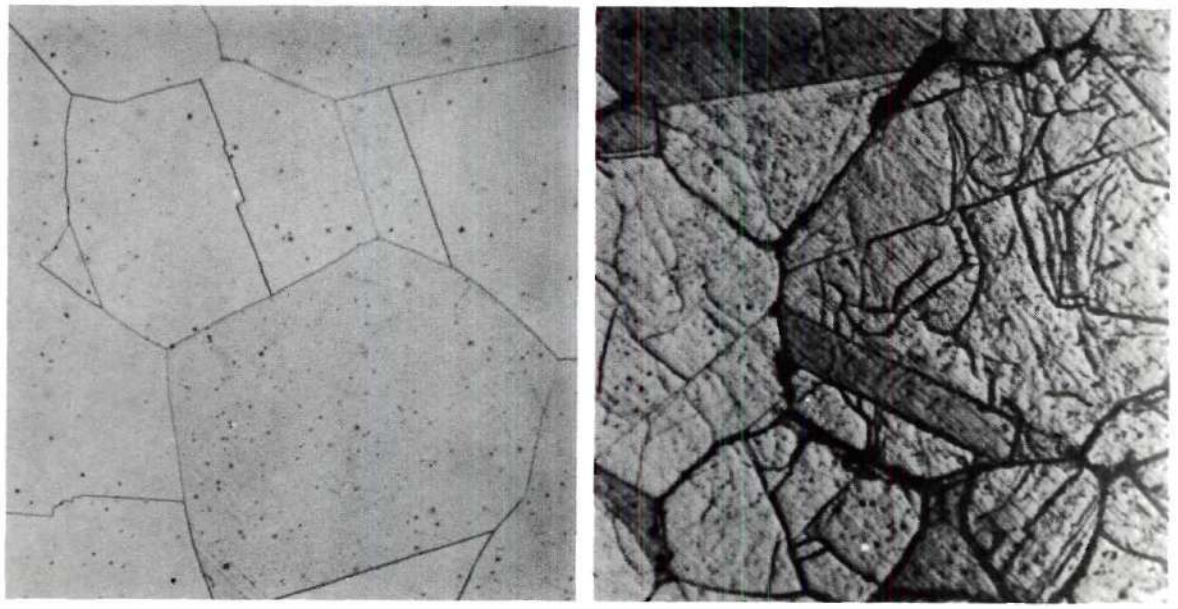

a. b.

Figure 1. CuPt As-Quenched and After Ordering. a. As-quenched 107X. b. Annealed 56 Hours at 300°C Showing Topographic Features.

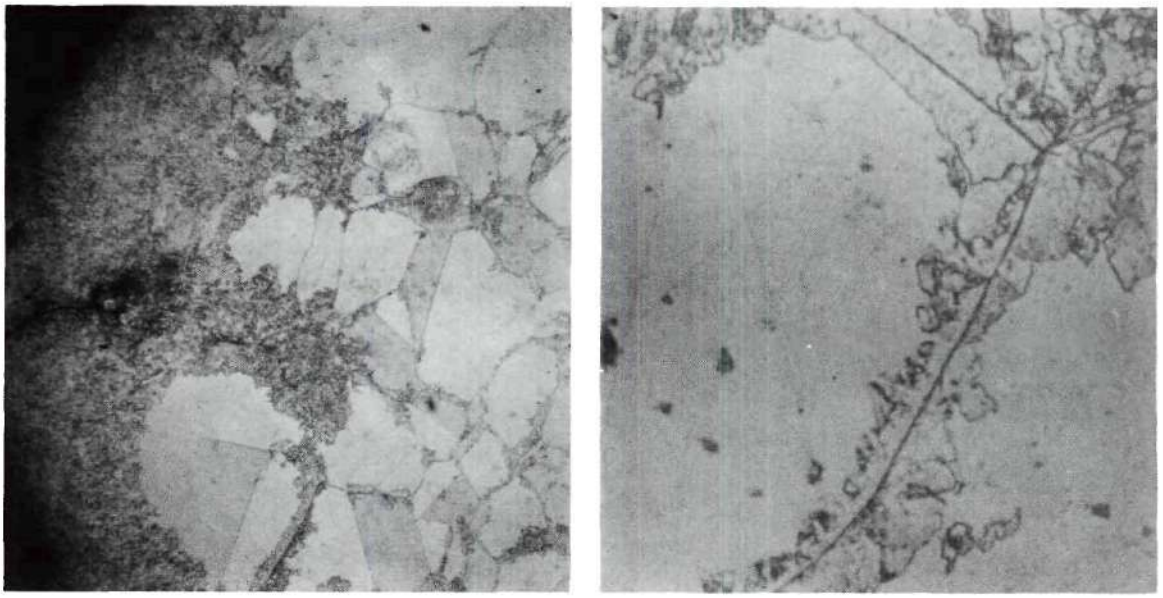

a. b.

Figure 2. CuPt Annealed at 300°C for 104 Hours. a. 30X b. 210X.

ordered domains. As is seen in Figure 2a, there are cracks associated with the surface component. These are seen after only a few minutes of annealing at 300 °C and 500 °C. Figure 3 shows examples of places where the grain boundary component appears on both sides of the original grain boundary. At 104 hours, at which time the heat treatments in this study were discontinued, there appeared to be no change in the centers of those grains not located near the sample surface.

At 700 °C the microstructure at first appears to be similar to that observed at the two lower ordering temperatures. At five minutes (Figure 4a) intergranular cracks appear at the surface of the sample. By ten minutes the boundaries have thickened and isolated portions of the grain boundary component appear (Figure 4b). From fifteen minutes onward the behavior differs from that of the 300 °C and 500 °C anneals. Figure 5 shows "flaring" and discontinuities at grain boundaries. By one hour, the general structure represented by Figure 6a is observed. The flares have become long needles which seem to be more profuse in grains near the surface and in grains near intergranular cracks. The needles are dense in some areas while totally absent in others. When they first appear, the needles are fine (Figure 6b) but as ordering time at 700 °C is increased they coarsen (Figure 6c) with some crossing entire grains. Figure 6c also shows a grain boundary component which may be equivalent to the grain boundary component observed after ordering anneals at 300 °C and 500 °C. Annealing the sample for 73 hours does not significantly change the microstructure. However, needles already present coarsen, as can be seen in Figure 7.

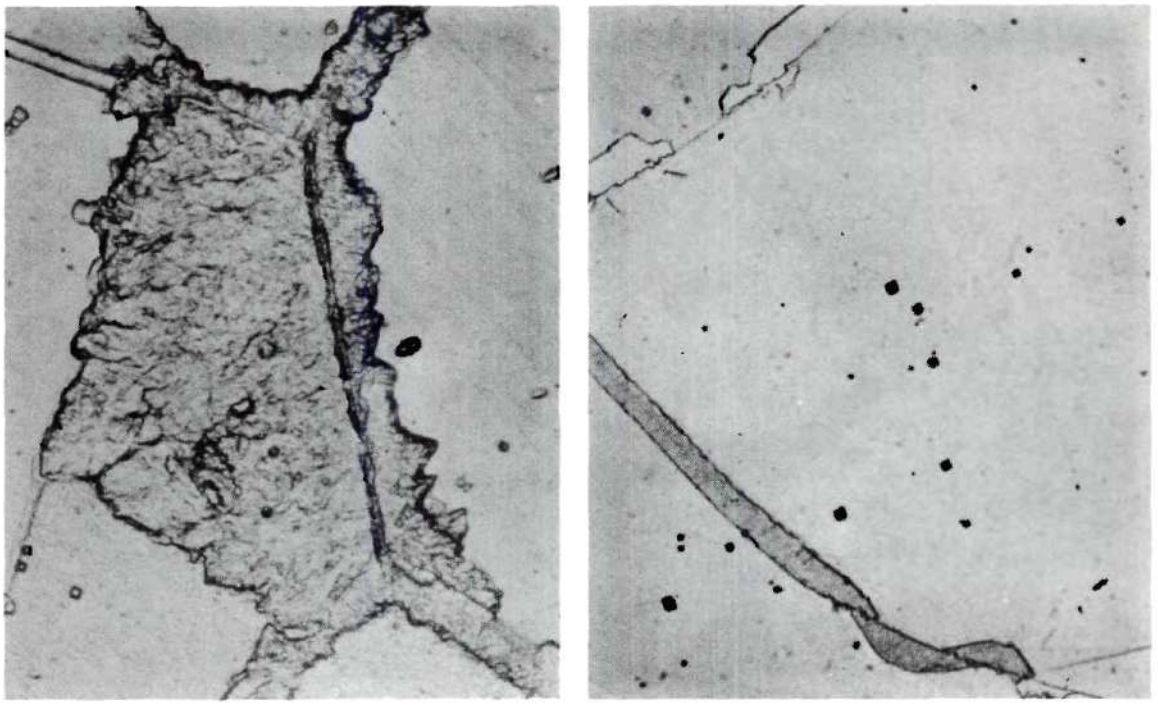

a. b.

Figure 3. Grain Boundary Components in CuPt. a. Annealed at 300°C for 56 Hours - 250X. c. Annealed at 500°C for 84 Hours - 260X.

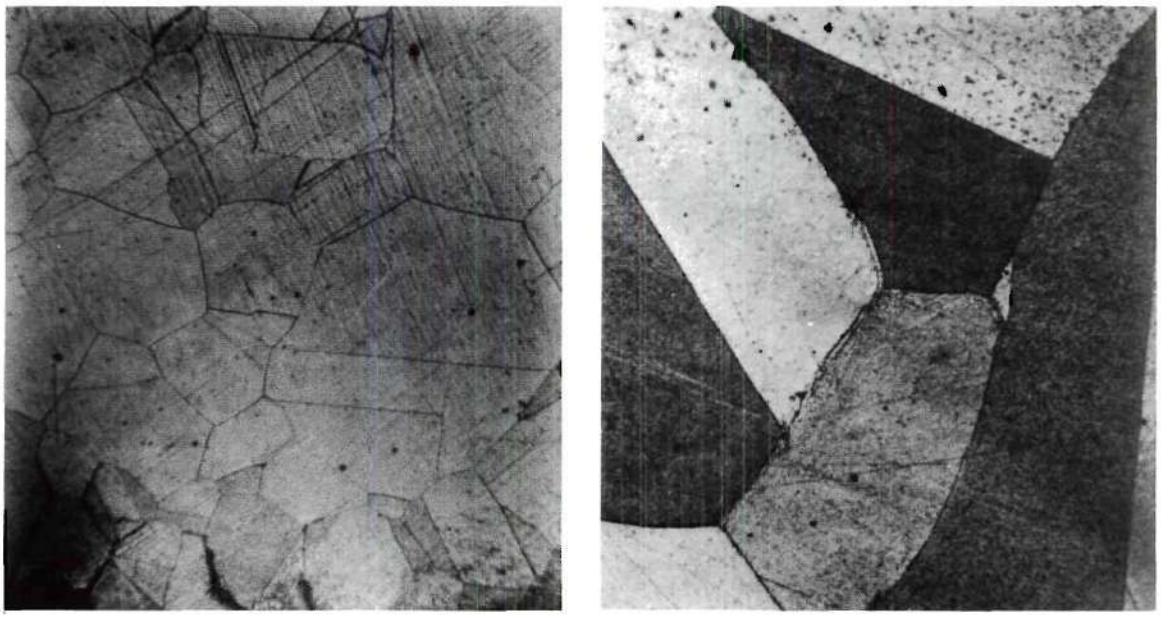

a. b.

Figure 4. CuPt Annealed at 700°C. a. Five Minutes - 29X. b. Ten Minutes - 230X.

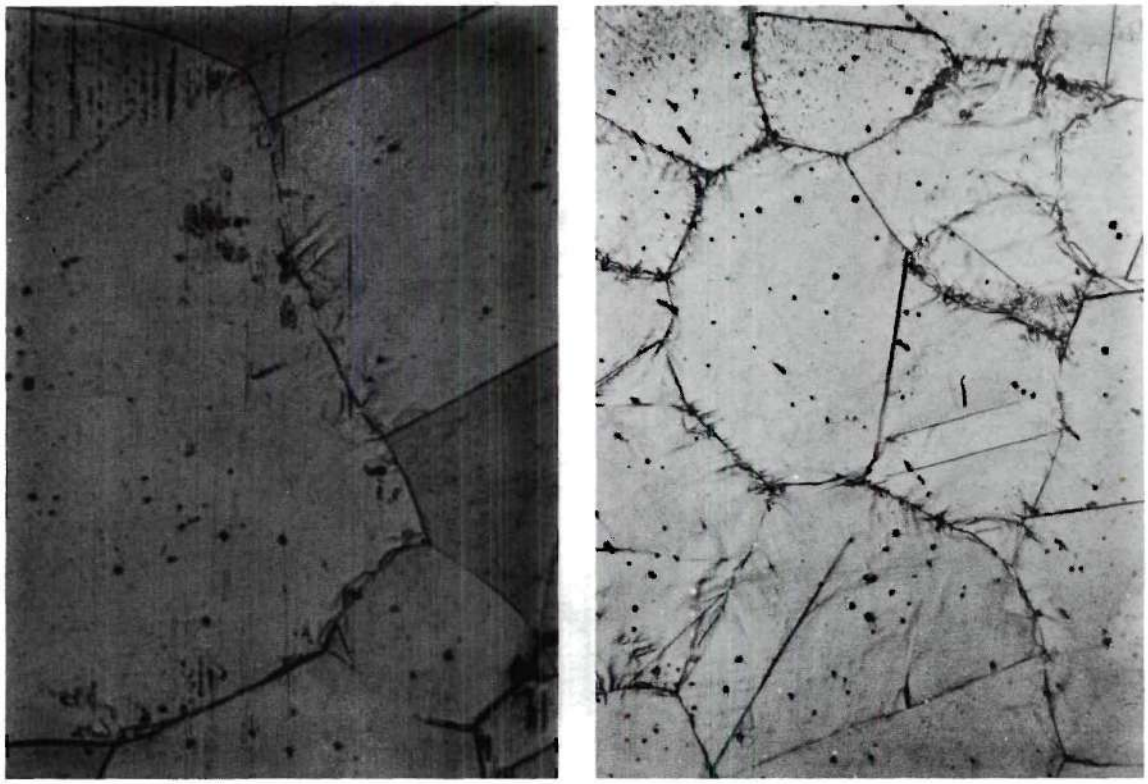

a. b.

Figure 5. CuPt Annealed at 700°C. a. Fifteen Minutes -240X, b. Thirty Minutes - 155X.

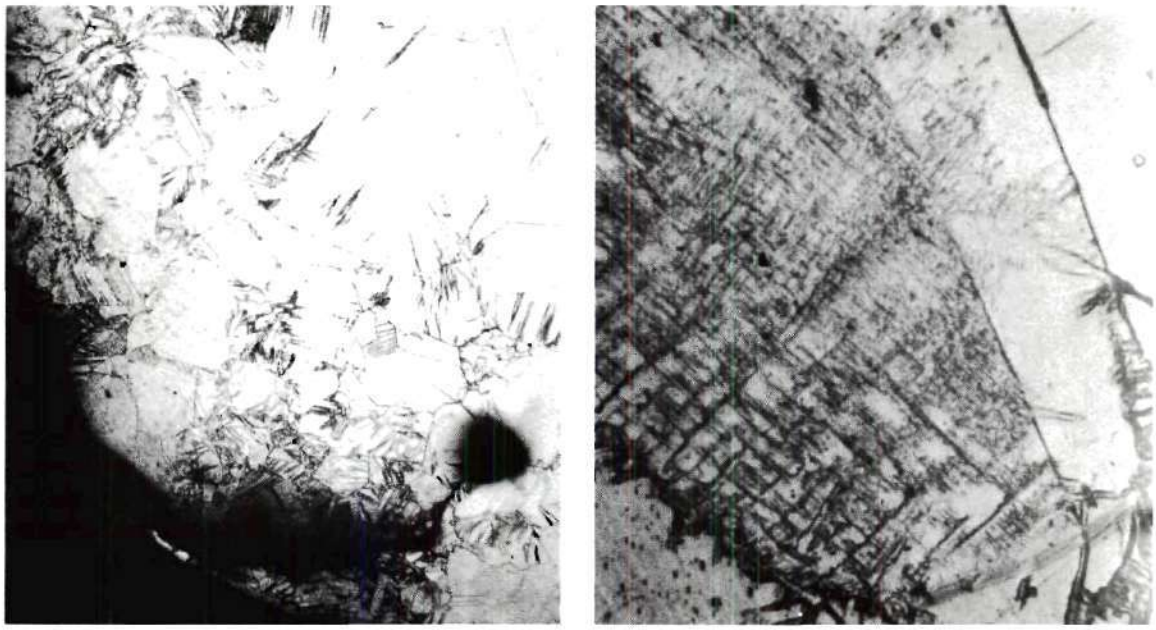

a.

b.

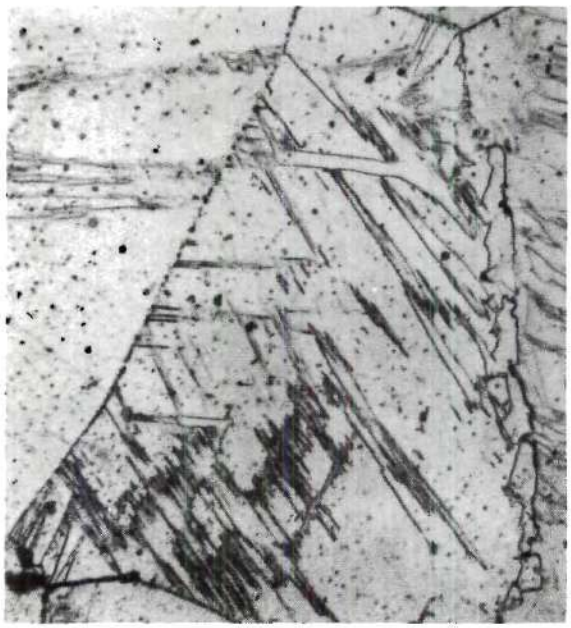

c.

Figure 6. CuPt Annealed at 700°C. a 16 Hours-28X. b. Two Hours-280X. c. Eight Hours-230X.

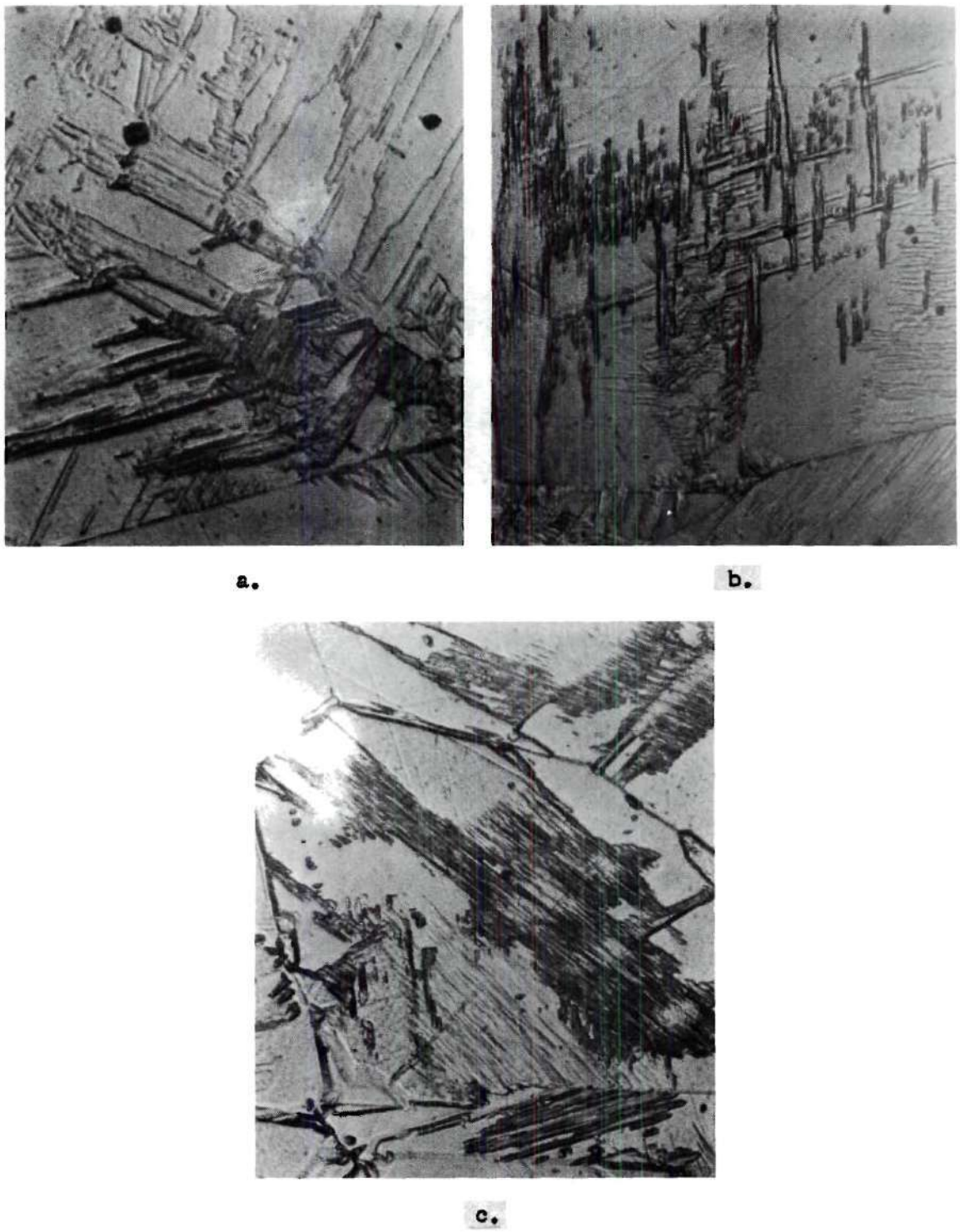

Figure 7. Twins in CuPt Annealed at 700°C for 73 Hours. a. 600X. b. 400X. c. 400X.

Hardness Test

Figure 8 shows plots of Knoop hardness numbers against annealing time for samples initially in the quenched state. Four plots are shown: 300°C to 104 hours, 500°C to 84 hours, 700°C to 73 hours, and 700°C to 20 minutes. These samples were used for the optical metallography described in the proceding section and were subsequently used for TEM studies. As can be seen from the figure, the as-quenched hardness varies from 165 to 190 reflecting the inability to obtain consistent quenches. Other quenched samples showed hardnesses in excess of 220. These, as mentioned previously, showed signs of extensive ordering and hence were not used for any of the ordering anneals. As-quenched hardnesses below 165 could not be obtained.

The 300°C anneal produced a slight initial hardening followed by a steady rise in hardness and then a small decrease in hardness at 50 hours. The behavior of the 500°C anneal was similar except that the intitial hardening is greater than for the 300°C anneal. The values of hardness in the graph for the 300°C and 500°C samples are average values for indentations made toward the center of the samples. Near the surface of these samples the "recrystallized" components predominate. As a result, the hardness is much different - on the average 100 Knoop hardness numbers below that of regions without the "recrystallized" component.

At 700°C two peak hardness values occurred, one at approximately six minutes and one at approximately 30 minutes. Gradual softening occurred from this point until the final hardness was less than that of the as-quenched state.

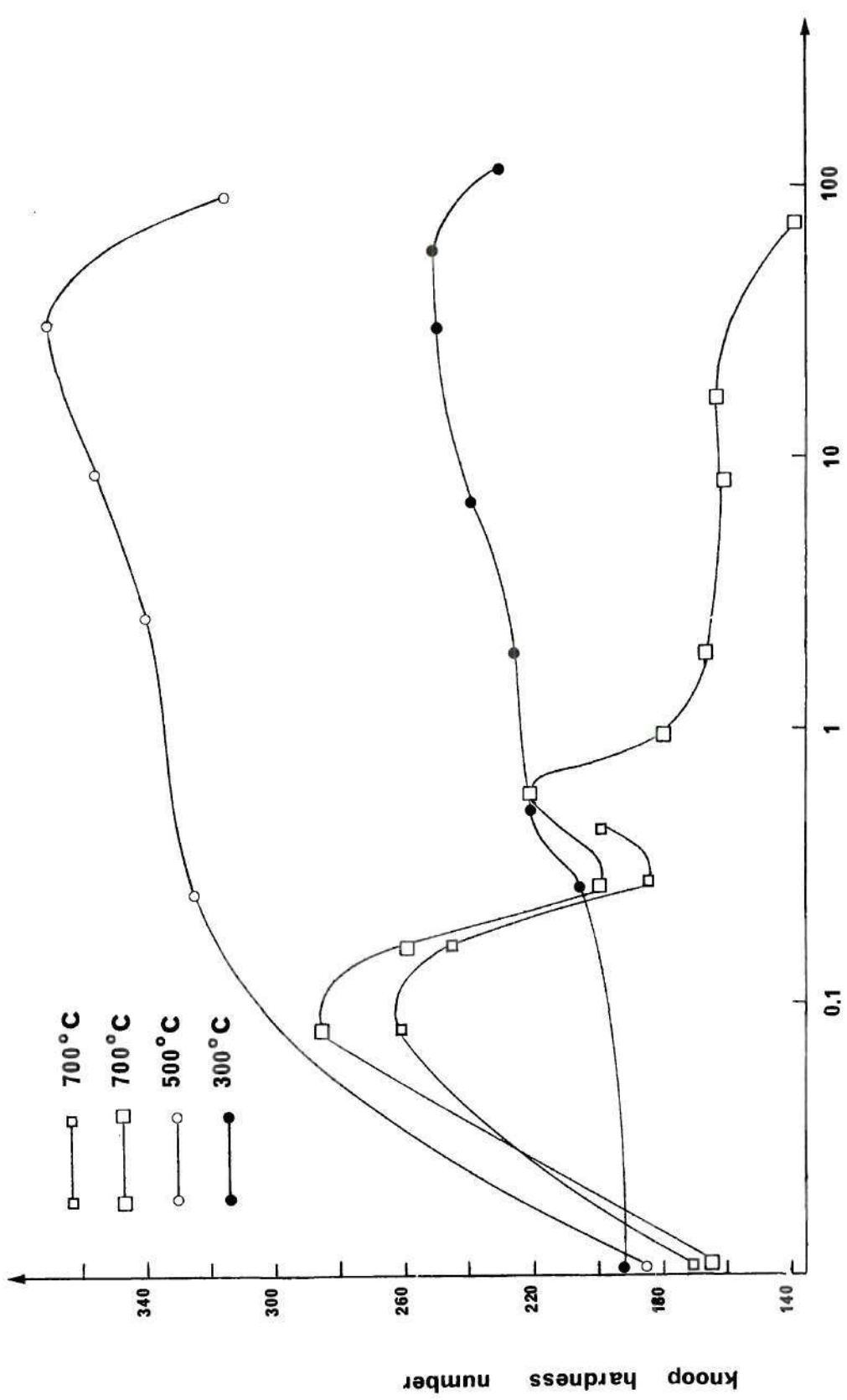

Figure 8. Hardness Versus Time for CuPt.

Transmission Electron Microscopy

Thin films were prepared from the hardness and optical metallography samples. Four different conditions were sampled: as-quenched, annealed at 300°C, annealed at 500°C, and annealed at 700°C.

The as-quenched sample with the lowest hardness (165) was selected since it represented the best quench. The diffraction patterns of this sample contained superlattice spots which correspond to two orientation variants of the ordered structure indicating that some degree of partial or short-range order was present. As discussed in Appendix I, a given diffraction pattern can contain a maximum of two of the four orientation variants. The two variants give no information about the two orientation variants which do not appear; they may or may not be present. By surveying the foil and looking at random diffraction patterns, it was found that the superlattice spots always corresponded to two orientation variants. This indicates that all four orientation variants are in the structure. The structure corresponding to the orientation variants could not be resolved. Figure 9a shows the dark-field image of the as-quenched foil using a (111) superlattice spot of Figure 9b. It can be seen that even using precision dark-field the domain structure is not resolved.

Preliminary examination of the 300°C and 500°C samples with TEM revealed that their structures were very similar to one another. To avoid duplication of results, it was decided to concentrate on observations of the 500°C sample. It was noted that specimens which were penetrated within the grains were very different from specimens which were near grain boundaries. This difference was not observed in

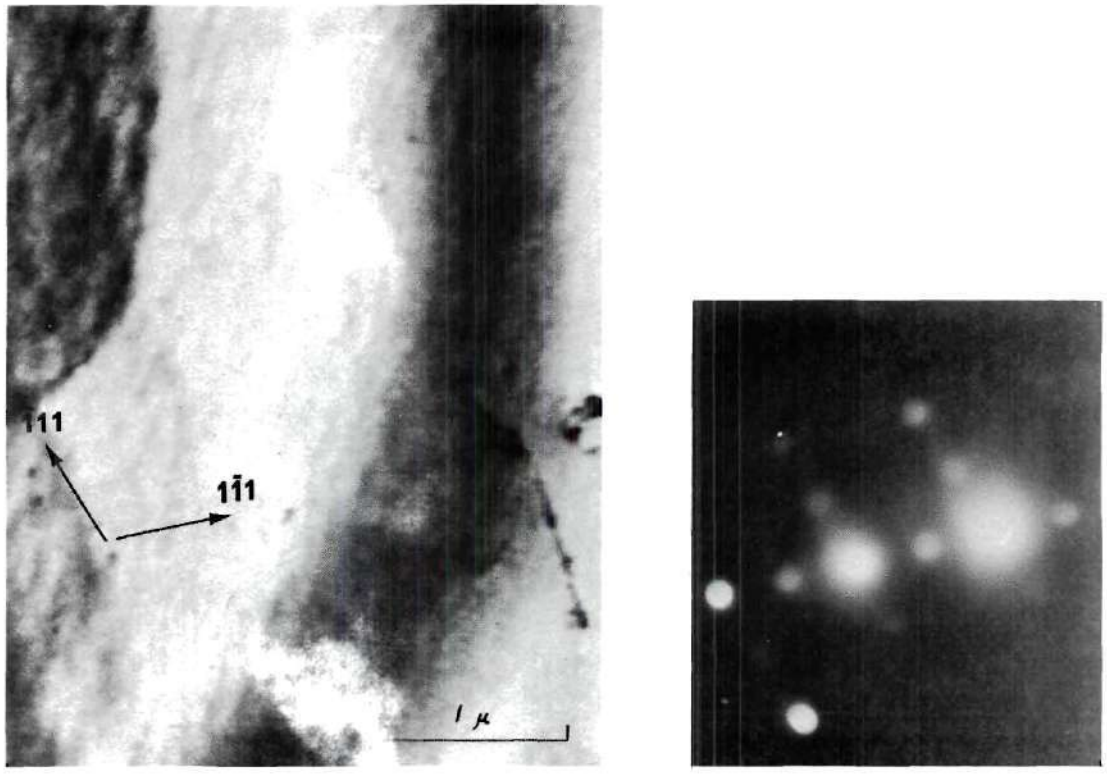

Figure 9. As-quenched CuPt. a. Dark-Field Using the (111) Reflection of b. b. Selected Area Diffraction Pattern of a. Having a (110) Orientation and Showing Superlattice Spots Corresponding to Two Orientation Variants.

as-quenched samples.

Within the grains (away from grain boundaries) a mottled structure containing all four orientation variants is observed. Figure 10a shows this mottled structure as it appears at 51 hours. The individual domains are not resolvable; striations within the mottled structure, however, can be seen. Trace analysis of several micrographs failed to reveal a consistent crystallographic orientation of the striations. Figure 10b shows the diffraction pattern of Figure 10a. Superlattice spots corresponding to two orientation variants are seen in the diffraction pattern. As has been argued for the as-quenched foils, the recurrence of two orientation variants in random diffraction patterns indicates that all four orientation variants are present within the structure. In addition, as is discussed in Appendix I, diffraction patterns which show multiple Laue zones contain superlattice spots corresponding to all four orientation variants. Continued heating to 84 hours results in a slight coarsening of the mottled structure with all four orientation variants still present. The coarsened mottled structure appears to be almost resolvable in thin areas where there are few overlapping nuclei.

The grain boundary and surface components which were observed optically appear in the electron microscope to be of similar microstructure. In both locations the structure was relatively featureless, containing no APB's, few dislocations and few twins. The diffraction patterns corresponding to these areas indicate that they are made up of only one orientation variant. Superlattice spots are either absent or are present for just one orientation variant indicating that the grain boundary and surface component is composed of but one orientation variant.

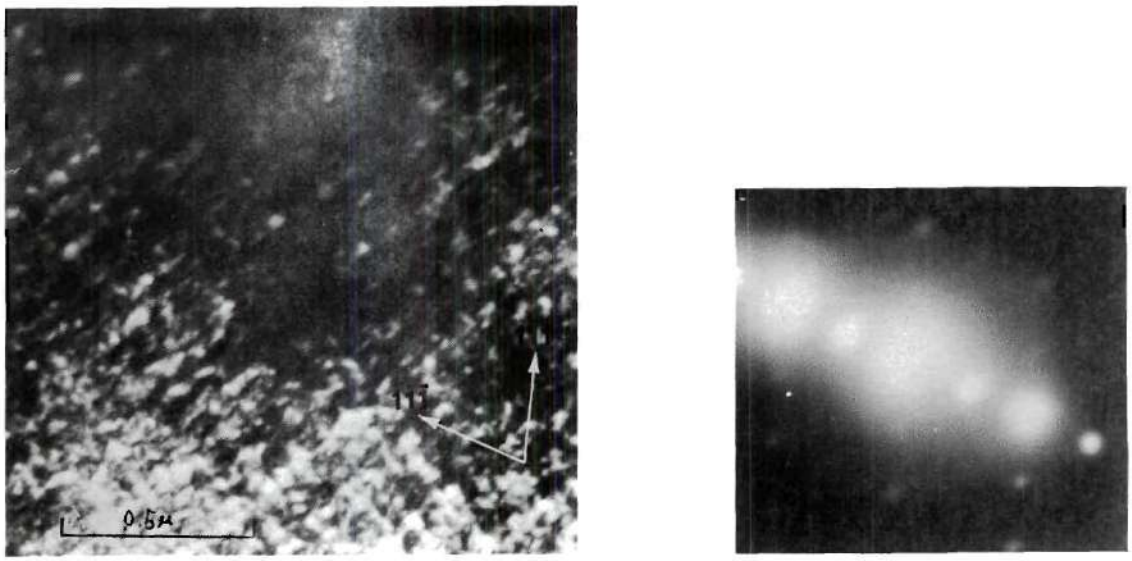

a. b.

Figure 10. Mottled Structure in CuPt Annealed at 500°C for 51 Hours. a. Bright-Field (110) Orientation. b. Selected Area Diffraction Pattern of a. Showing (110) Orientation and Superlattice Spots of Two Orientation Variants.

Figure 11a shows areas of the grain boundary component with subgrain boundaries and a twin. This figure not withstanding, few twins are observed in the grain boundary component.

The preferential attack at grain boundaries made it difficult to obtain foils which were thin both at mottled areas and at the grain boundary and surface components. Thus, it was difficult to ascertain the nature of the boundaries between the two structures. Figures 12 and 13 show two such interfaces at a grain boundary. Figure 12 shows one interface with the mottled structure above and the grain boundary component below, while Figure 13 shows the other interface with the mottled structure below. Selected area diffraction patterns of the two structures show that the fundamental pattern changes across one interface (Figure 13) but remains that same across the other (Figure 12). Hence, the former interface is incoherent while the latter is coherent. In traversing the coherent interface (Figure 12) the number a visible variants in the patterns changed from two in the mottled structure to one in the grain boundary component as expected.

Because of their more rapid variations in hardness, the 700° C samples were viewed at more frequent annealing intervals. At five minutes the samples show a fine mottled structure throughout. Figure 11b shows this structure at a grain boundary. As in the mottled structure observed at 300° C and 500° C all four orientation variants make up the 700° C mottled areas.

At 12 minutes at 700° C the mottled structure has disappeared but many other features are seen. Figure 14 shows a structure a little coarser than the original mottled structure. Close examination reveals

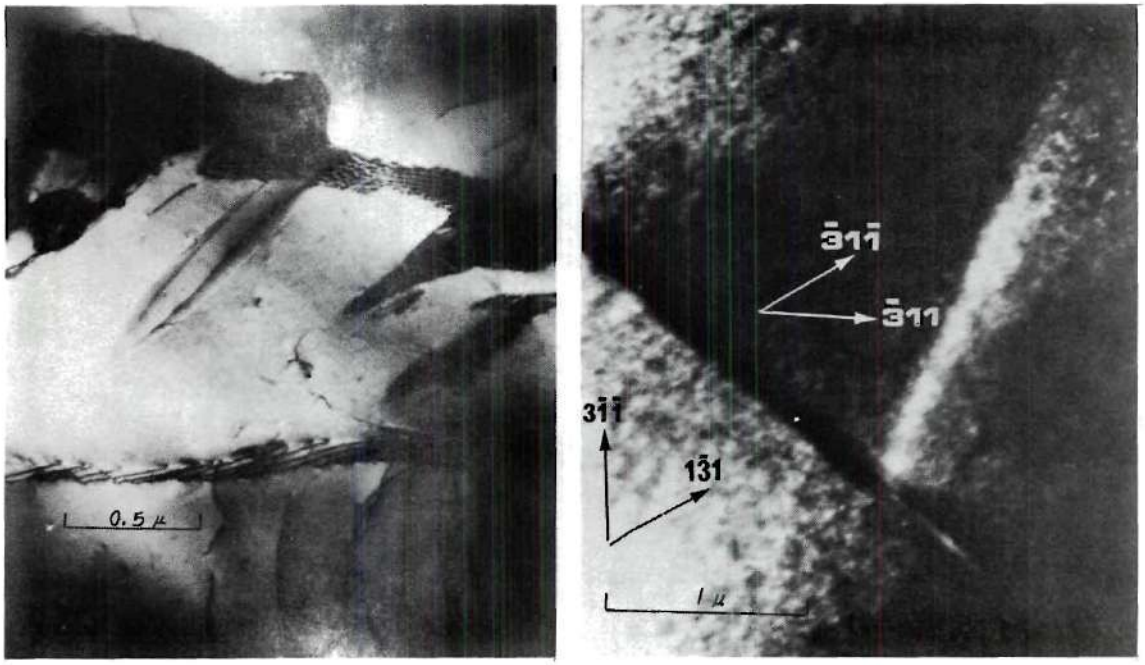

a. b.

Figure 11. Near the Grain Boundary at 500°C and at 700°C. a. Grain Boundary Component in CuPt Annealed at 500°C for 51 Hours. b. Mottled Structure in CuPt Annealed at 700°C for Five Minutes.

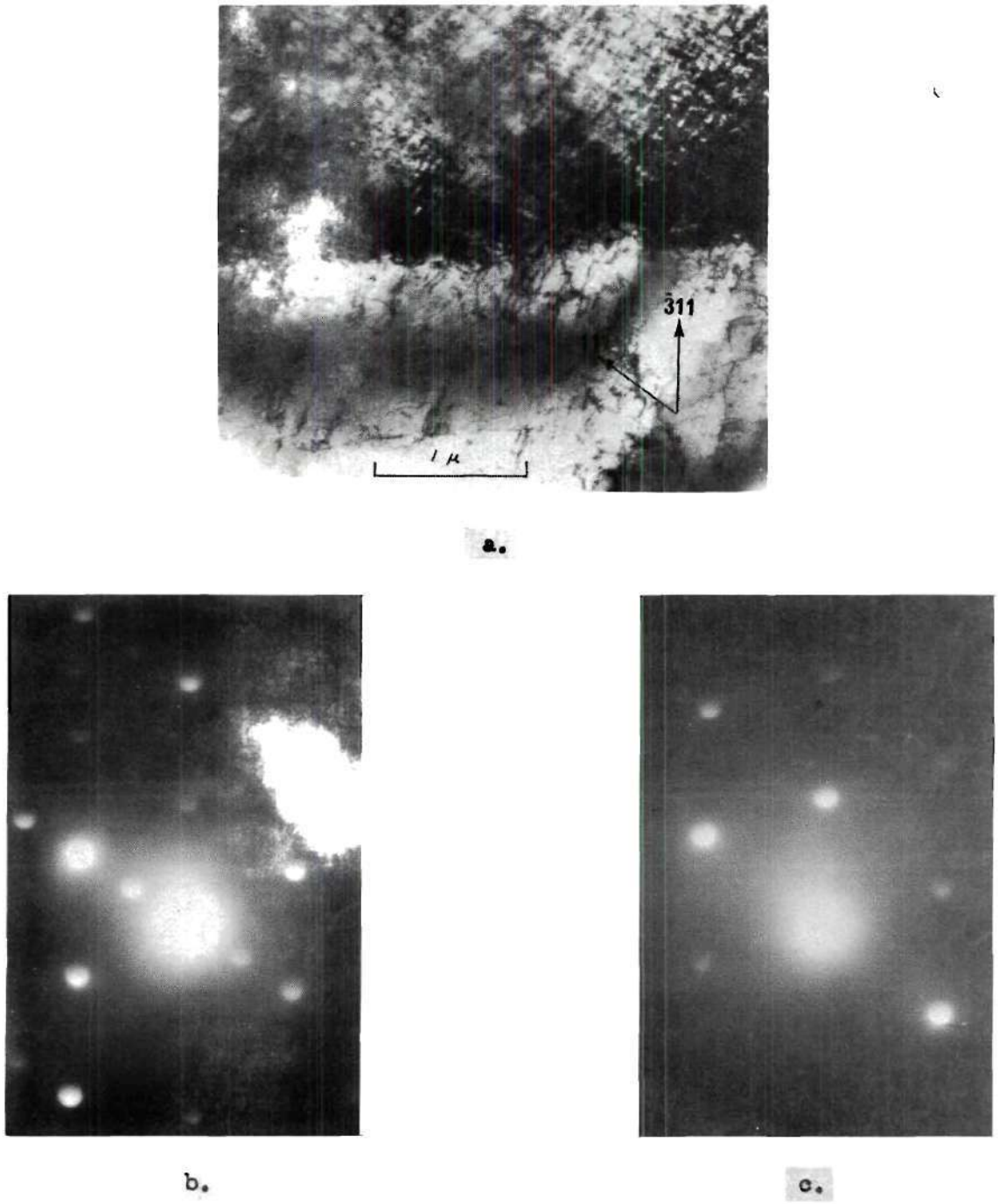

Figure 12. A Boundary Between Grain Boundary Component and Mottled Structure in CuPt Annealed at 500°C for 84 Hours. a. Bright Field. b. Diffraction Pattern Taken Inside Mottled Area of a. Showing (112) Orientation with Superlattice Spots Corresponding to Two Orientation Variants. c. Diffraction Pattern Taken Inside Grain Boundary Component of a. Showing (112) Orientation with Superlattice Spots Corresponding to One Orientation Variant.

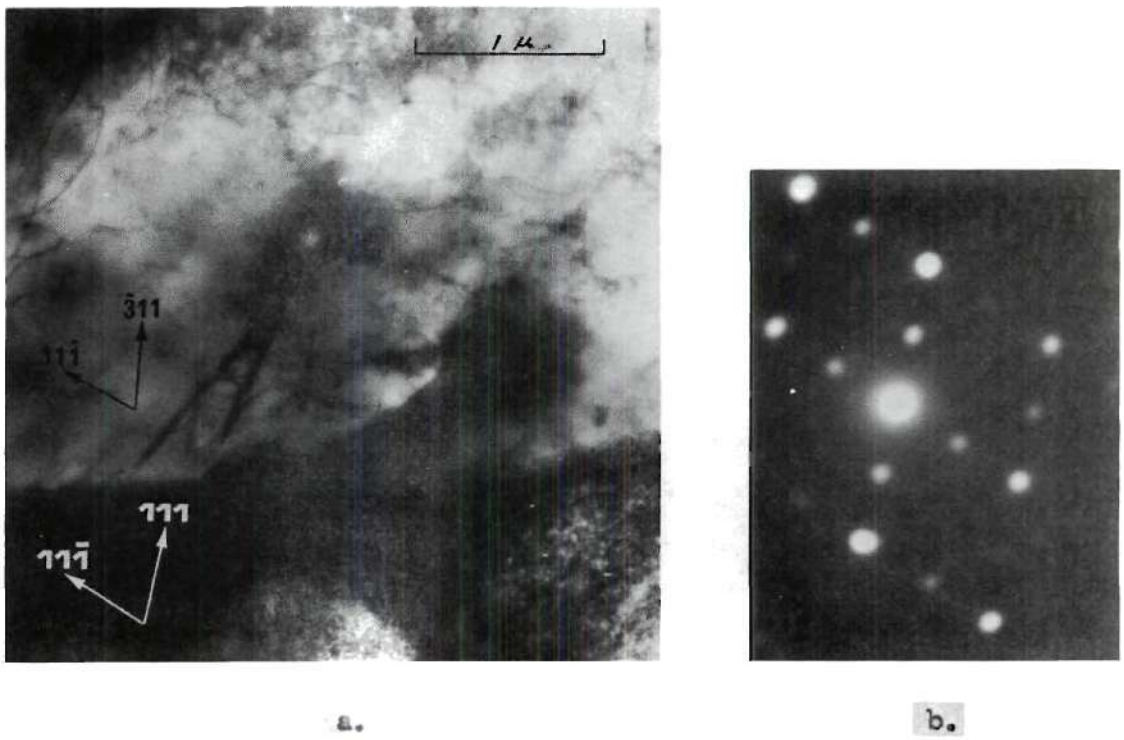

Figure 13. A Boundary Between Grain Boundary Component and Mottled Structure in CuPt Annealed at 500°C for 84 Hours. (Lower Boundary of Grain Boundary Component of Figure 18a.) a. Bright-Field. b. Diffraction Pattern Taken Inside Mottled Area of a. Showing $(1\bar{1}0)$ Orientation with Superlattice Spots Corresponding to Two Orientation Variants. (The Grain Boundary Component has the Same Diffraction Pattern as Figure 18c).

lamellae which run in at least two directions. Assuming these lamellae to be planar features, analysis of many micrographs show that they lie parallel to $(01\bar{1})$ and (100) habit planes which are twin planes for this system. The diffraction pattern (Figure 14b) shows a single fundamental pattern and only one set of superlattice spots, suggesting that there can be no more than three orientation variants present. Indexing the spots added by the first Laue zones above and below the plane of reflection in Figure 14d that three orientation variants are present. Figure 15 shows an area similar to that of Figure 14 at a higher magnification. Twins on three habit planes are seen: (100), $(01\bar{1})$ and (010). The majority are of the (100) and $01\bar{1})$ types and correspond to orientation variants type two and type four as described in Appendix II. The remaining (010) habit plane could result from the intersection of type one and type four variants giving a total of three variants present in the microstructure.

Figures 14 and 15 show areas that have developed directly from the mottled structure. Other areas of the 12 minute sample have coarsened past the stages of these micrographs. Figure 16 shows a region in the 700°C sample at 12 minutes in which the twinning has thinned out. Using the (111) superlattice reflection of Figure 16b the dark-field picture of Figure 16c was obtained. Both twin directions appear bright. Since the (111) superlattice spot originates in only one orientation variant both twin directions must correspond to the same variant. Indexing these twins, one finds their habit planes to be (100) and $(01\bar{1})$. Again, using the notation of Appendix II, these are habit planes formed by the type two and type four orientation variants. The matrix of

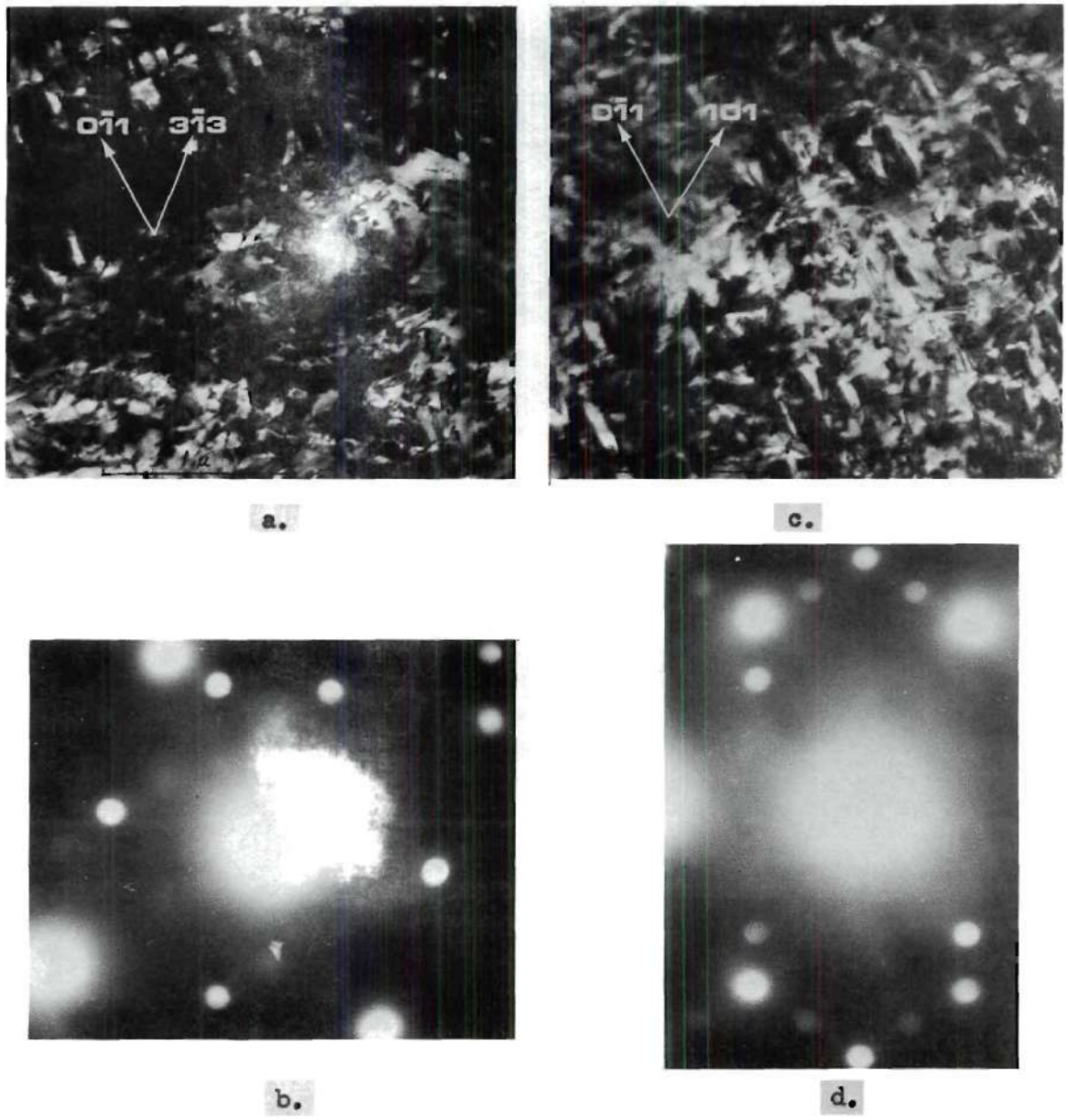

Figure 14. Densely Twinned Structure in CuPt Annealed at 700°C for 12 Minutes. a. Bright-Field Showing Twins with (100) and (01$\bar{1}$) Twin Planes. b. Selected Area Diffraction Pattern of a. Showing (333) Orientation with Superlattice Spots Corresponding to One Orientation Variant. c. Bright-Field of a. After Tilting. d. Selected Area Diffraction Pattern of c. Showing ($\bar{1}$11) Orientation Plus Superlattice Spots from First Laue Zone Corresponding to Three Orientation Variants.

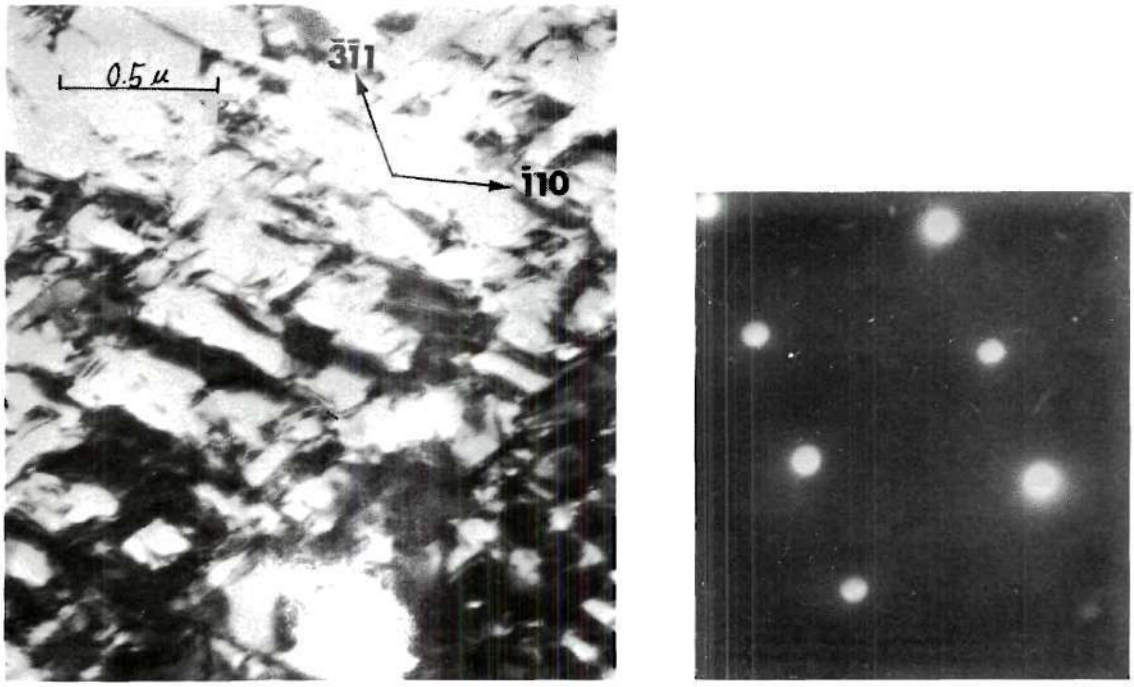

Figure 15. A Densely Twinned Area in CuPt Annealed at 700°C for 12 Minutes. a. Bright-Field Showing Twins on (100), (0$\bar{1}$1), and (010) Habit Planes. b. Selected Area Diffraction Pattern of a. Showing (114) Orientation with Superlattice Spots Corresponding to One Orientation Variant.

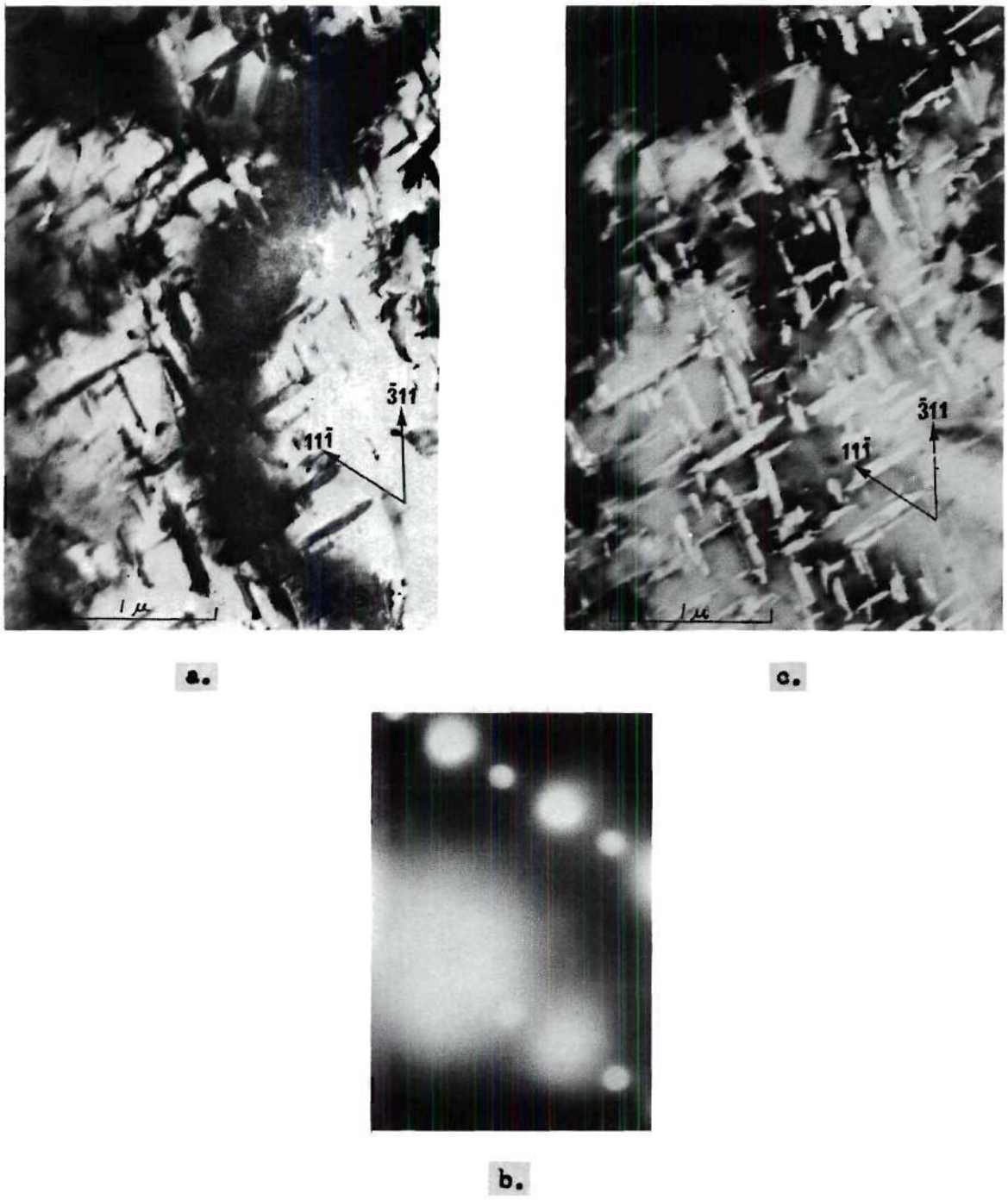

Figure 16. Twins in CuPt Annealed at 700°C for 12 Minutes. a. Bright-Field Showing Twins with (100) and (01$\bar{1}$) Twin Planes. b. Selected area Diffraction Pattern of a. Showing (112) Orientation with Superlattice Spots Corresponding to One Orientation Variant. c. Dark-Field of a. Using (111) Superlattice Reflection of b. Showing both (100) and (011) Bright.

Figure 16 is of one orientation variant and both twin directions are of the other orientation variant.

Structure like those in Figure 16 are common at 12 minutes. In general, only two orientation variants are present in any given area of the structure. One variant is the matrix and the other is that of the twins whose twin plane is either one or both of the possible twin planes given for the intersection of two orientation variants in Appendix II. Figure 17 shows an example of continued coarsening of another area of the 12 minute sample. Here there is only one twin plane, the (100). It will be noted that in Figure 17a the twins are dense. As the field of view is moved to the right in Figures 17b and 17c, the twins thin out until finally there are no twins. In between the thinning twins and in regions which show no twins are networks of APB's. Interestingly, the APB's in Figure 17c tend to lie in the same directions as the neighboring twins.

In some areas of the 700°C sample which was annealed for 12 minutes the coarsening has proceded even further. In these areas there is no twinning, and hence, only one orientation variant. Instead, there are dense networks of APB's. Figure 18a is a dark-field micrograph of APB's using the (311) superlattice reflection of the diffraction pattern in Figure 18b.

In samples which have been annealed at 700°C for 20 minutes, the twins have coarsened still further. They are fewer in number but longer in length. As are those at 12 minutes, the 20 minute twins are made up of one orientation variant which can have two different twin planes with respect to the matrix which is made up of another single orientation

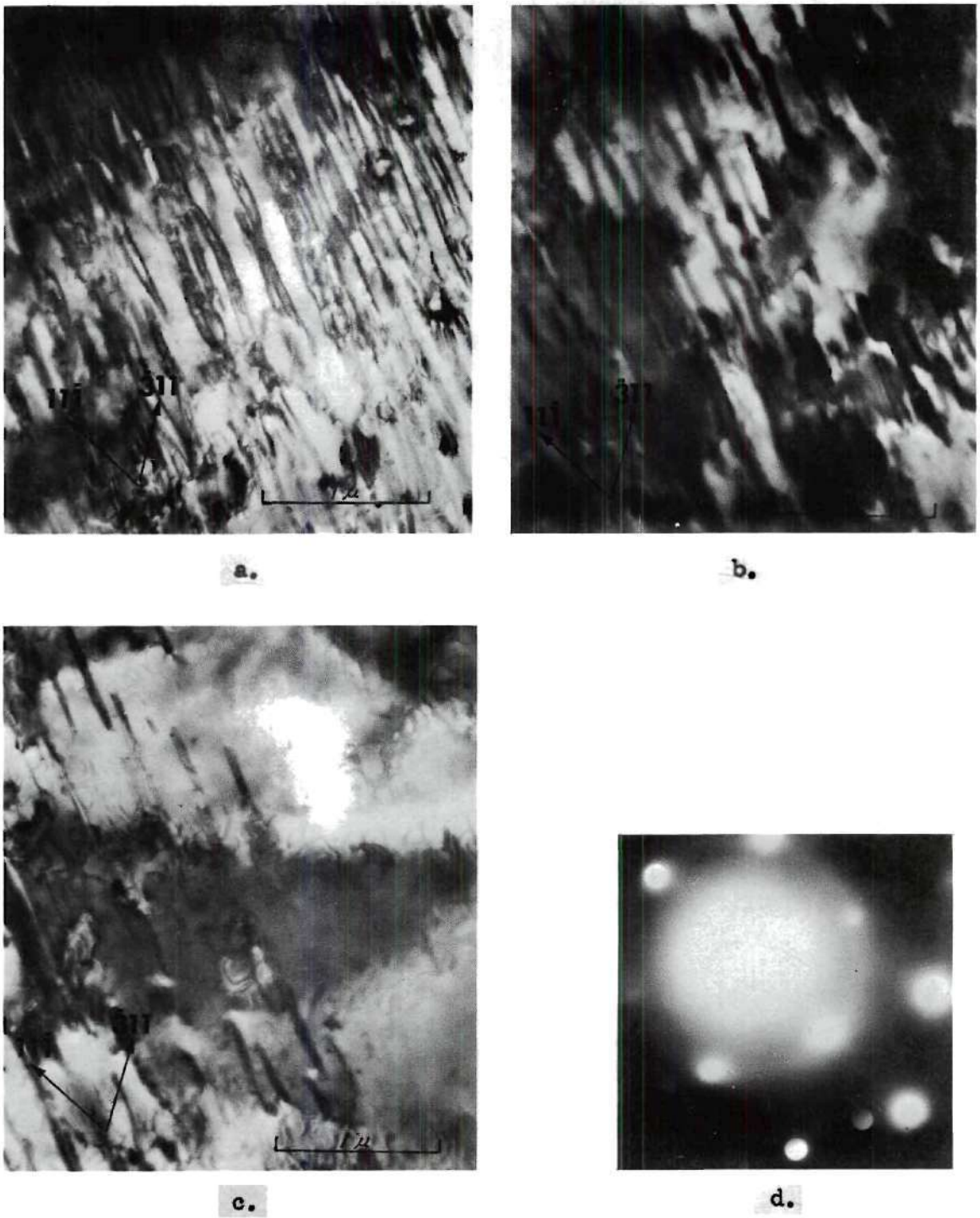

Figure 17. Thinning out of Twins in CuPt Annealed at 700°C for 12 Minutes. a. Bright-Field Showing Twins with (100) Twin Planes. b. Area to the Right of a. c. Area to the Right of b. d. Selected Area Diffraction Pattern Showing (112) Orientation and Superlattice Spots Corresponding to One Orientation Variant.

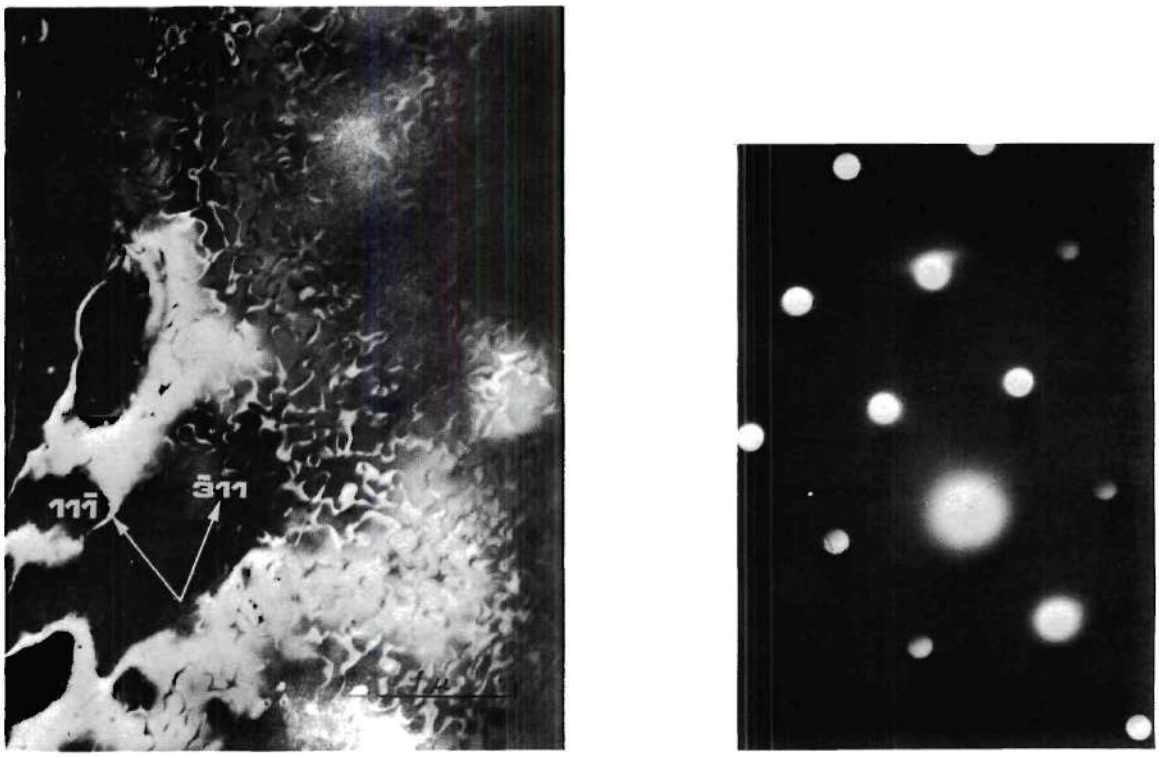

a. b.

Figure 18. Antiphase Domain Boundaries in CuPt Annealed at 700°C for 12 Minutes. a. Dark-Field Using (311) Superlattice Reflection. b. Selected Area Diffraction Pattern of a. Showing (112) Orientation with Superlattice Spots Corresponding to One Orientation Variant.

variant. At twin boundaries, strong δ-fringe contrast is observed. Figure 19 shows (100) twins with δ-fringe contrast indicative of localized interface strain between the two orientation variants. Between the twins in Figure 18 dim APB contrast is noted. It is not possible from this and other micrographs of the 700°C sample annealed for 20 minutes to detect growth of the APD's from their size at 12 minutes. In fact, at both 12 and 20 minutes antiphase domain size seems to be strongly dependent on the particular portion of the foil being viewed. When the appear between twin, APD's are smaller than in areas which are lightly twinned or nontwinned.

When the 700°C sample is annealed to 73 hours, the twinned structure which appears in the optical microscope is seen in the electron microscope. The twins are long and generally extend beyond the thinned area of the foil. They appear in clusters and tend to run in the same direction so that in a given field of view in the electron microscope one sees only one twin plane. As at 12 and 20 minutes, the habit plane of the twins is {100} or {110}. The thickness of the twins varies from approximately less than a tenth of a micron to dimensions that extend beyond the field of view at 20,000X in the electron microscope. The twins at 12 and 20 minutes at 700°C are lenticular; those at 73 hours have nearly parallel edges. The twin boundaries at 73 hours show distinct δ-fringe contrast. Dislocation tangles and pile-ups appear at these boundaries in many cases. Although these long lamellar twins are prominent in CuPt annealed at 700°C for 73 hours, the greater part of the foil shows no twin boundaries at all. Unless the sample is mishandled, these areas show few dislocations. These areas are composed of a single

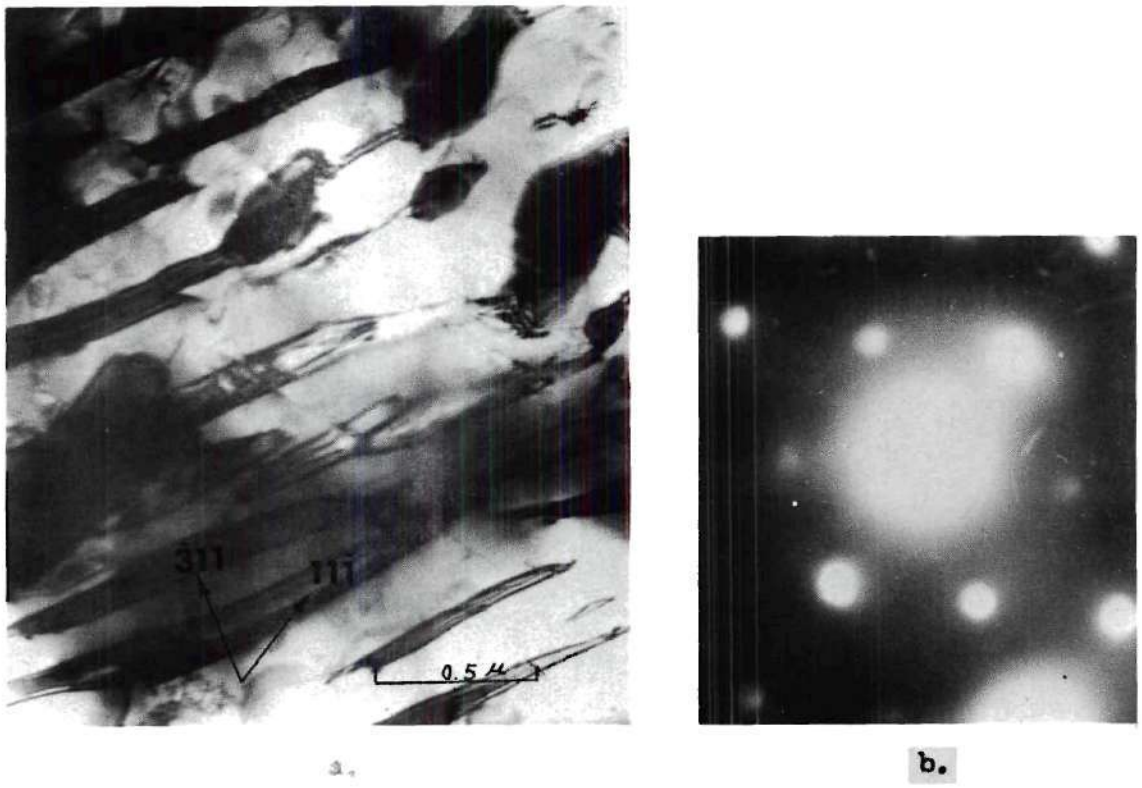

Figure 19. Twins in CuPt Annealed at 700°C for 20 Minutes. a. Bright-Field Showing Twins with (100) Twin Planes. b. Selected area Diffraction Pattern of a. Showing (112) Orientation with Superlattice Spots Corresponding to One Orientation Variant.

orientation variant, and within them no APB contrast was detected. Moreover, APB contrast is not observed anywhere in the foil annealed for 73 hours at 700° C.

CHAPTER IV

DISCUSSION OF RESULTS

The kinetics and mechanism of ordering depends on the sequence of the various quenches and anneals. The quench into icy brine from above T_c has proved to be a very critical step in the sequence. Electron diffraction of the as-quenched samples shows superlattice spots. This indicates that the as-quenched samples are partially ordered, and contain a high density of nuclei from which the transformation can proceed. In addition, as the samples are heated to either 300°C, 500°C or 700°C, more nuclei develop as the samples pass through the low temperature ranges where rapid nucleation occurs. Thus the results of this study are expected to be different from those of a study such as Tanner's of Ni_2V (7) in which the sample has been quenched to the isothermal annealing temperature from above T_c. The difference is that in an approach such as Tanner's the mottled structure might never be seen at the higher annealing temperatures. This mottled structure results from rapid nucleation during the quench or during reheating. It is expected that isothermal anneals at 300°C and 500°C will produce mottled structure in any case, because at these temperatures rapid nucleation should occur.

The following observations have been made in this study of the ordering transformation in CuPt.

(i) At low temperatures (300°C and 500°C) the mottled structure occurs in the initial stages of ordering and persists with little

coarsening until it is replaced through growth of the structural component originating at the grain boundaries. The mottled structure consists of all four ordered variants whereas the grain boundary component consists of large domains of a single variant.

(ii) Surface "recrystallization" associated with ordering at low temperatures is actually a continuation of the same microstructure observed in the grain boundary component. The grain boundary component replaces the mottled structure through growth by a grain boundary migration mechanism.* The surface component may be formed by direct domain coarsening or by grain boundary migration.

(iii) At high temperatures (700°C) the mottled component coarsens into a structure consisting of well-defined twins of different orientation variants lying on {100} and {011} type planes. The twinned component develops more rapidly near grain boundaries. The number of variants in any given area eventually decreases to two with the formation of large twins several microns in length. Antiphase domains within the twins and in the matrix eventually coarsen to such a size that APB's are no longer observed.

(iv) Strains associated with the ordering process are severe enough to cause grain boundary cracking.

The observed relationships between the transformation and order hardening in this alloy are as follows:

(i) At 500°C and 700°C the hardness increases rapidly with the appearance of the mottled structure. At 300°C the hardness increases

*Subsequent work by Paris (57) has shown that if the CuPt alloy is annealed at 500°C for 1000 hours the grain boundary component sweeps through all of the mottled structure thus completing the ordering.

less dramatically with the appearance of the mottled structure.

(ii) At low temperatures (300°C and 500°C) the hardness drops with the growth of the grain boundary and surface components. Selective microhardness measurements show that this coarse-domained microstructure is distinctly softer than the mottled structure.

(iii) At 700°C dual hardening is observed. The hardness peaks first as the mottled structure begins to coarsen into twins of two or three orientation variants and shows a smaller second peak as the twins continue to coarsen. As time continues the hardness eventually drops to less than that of the as-quenched state. In the final overaged state the twins and antiphase domains are generally larger than one micron.

The following topics regarding the transformation and its relationship to the hardening will be discussed in some detail: (i) the driving force and mechanisms for ordering at high and low temperatures; (ii) the significance of the grain boundaries and free surfaces in the formation of the coarse-domained "recrystallized" component; (iii) the hardness mechanisms associated with the various microstructures - in particular the origin of the secondary hardening at 700°C.

The important parameters of neostructural ordering transformations have been discussed in detail by Southworth and Ralph (9). In addition to the normal free energy terms associated with the volume and surface of newly formed nuclei, the transformation is severely affected by associated strains. Since the dimensions of the lattice are a function of the degree of order (43) the formation and growth of ordered nuclei of different variants must result in localized and long-range strain fields which oppose the transformation. The

development of intergranular cracking is a manifestation of such strains. X-ray measurements in Ni_4Mo (23) have shown that strains do vary with degree of order and domain size and are quite large when the domain size is fine, as in the mottled region of ordered CuPt.

Since the mottled region in CuPt was not clearly resolved in the TEM its exact structure is not known. It might consist of (a) ordered domains in a "disordered" matrix, (b) a uniform partially ordered structure of small impinging domains or (c) domains with diffuse boundaries producing periodic variations in order (15). In any case one can readily deduce from the micrographs and diffraction patterns that this component is made up of very small domains (less than 50 Å) of all four orientation variants.

The progress of the ordering at 300° C and 500° C is severely retarded by the accompanying lattice strains. It appears that the lattice reaches a metastable equilibrium at a very early stage with respect to domain size and degree of order. Electron micrographs show that the domain size does not coarsen measurably even with prolonged annealing (84 hours - 500° C). X-ray studies by Paris (57) at 500° C show that the degree of order within the mottled structure remains low (about 0.3) even as it is being consumed by the "recrystallized" component. These same x-ray measurements show that the coarser domained "recrystallized" component is highly ordered (approaching S=1). Thus, the ordering transformation at low temperatures is completed by the growth of the "recrystallized" component into the mottled structure.

From the above observations it seems clear that the ΔF of ordering is part of the driving force behind the growth of the "recrystallized"

component. The fact that the component forms initially at grain boundaries and free surfaces indicates that relief of ordering strains is also a part of the driving force. This seems all the more reasonable when it is realized that the transformation cannot progress further if the strains remain high or continue to build. The accumulated evidence of the optical and TEM micrographs indicates that the mechanism of growth is grain boundary migration. A recent experiment by Paris (57) has shown conclusively that the high angle grain boundaries actually do migrate during the transformation.* If the local strain on either side of a grain boundary is greatly different, strain energy is decreased if the less strained grain grows at the expense of the other (as in the strain-induced grain boundary migration mechanism of Cahn (35). Besides reducing the strain, the migrating grain leaves ordered material (the grain boundary component) in its wake. Thus, this process is promoted by the change in free energy due to strain and due to ordering. The features in the optical micrographs showing the "recrystallized" component may be explained in terms of the model illustrated in Figure 21. It is possible for a penisula to migrate, as in Figure 21a, to form an island or, as in Figure 21b, to form grain boundary component on either side of a grain boundary.

One would expect the "recrystallized" component near the surface to be of a similar nature to the grain boundary component since they are

*A partially ordered sample showing the grain boundary component was subsequently disordered for a short time above T_c. The "recrystallized" areas appeared as parts of neighboring grains (see arrows in Figure 20). By disordering the sample, etching affects associated with coarse ordered domains were eliminated.

Figure 20. Grains in CuPt Which after Annealing at 500°C for 100 Minutes was Annealed at 850°C for Seven Minutes and then Quenched with Ice Brine-140X. (Micrograph courtesy of Mr. H. Paris).

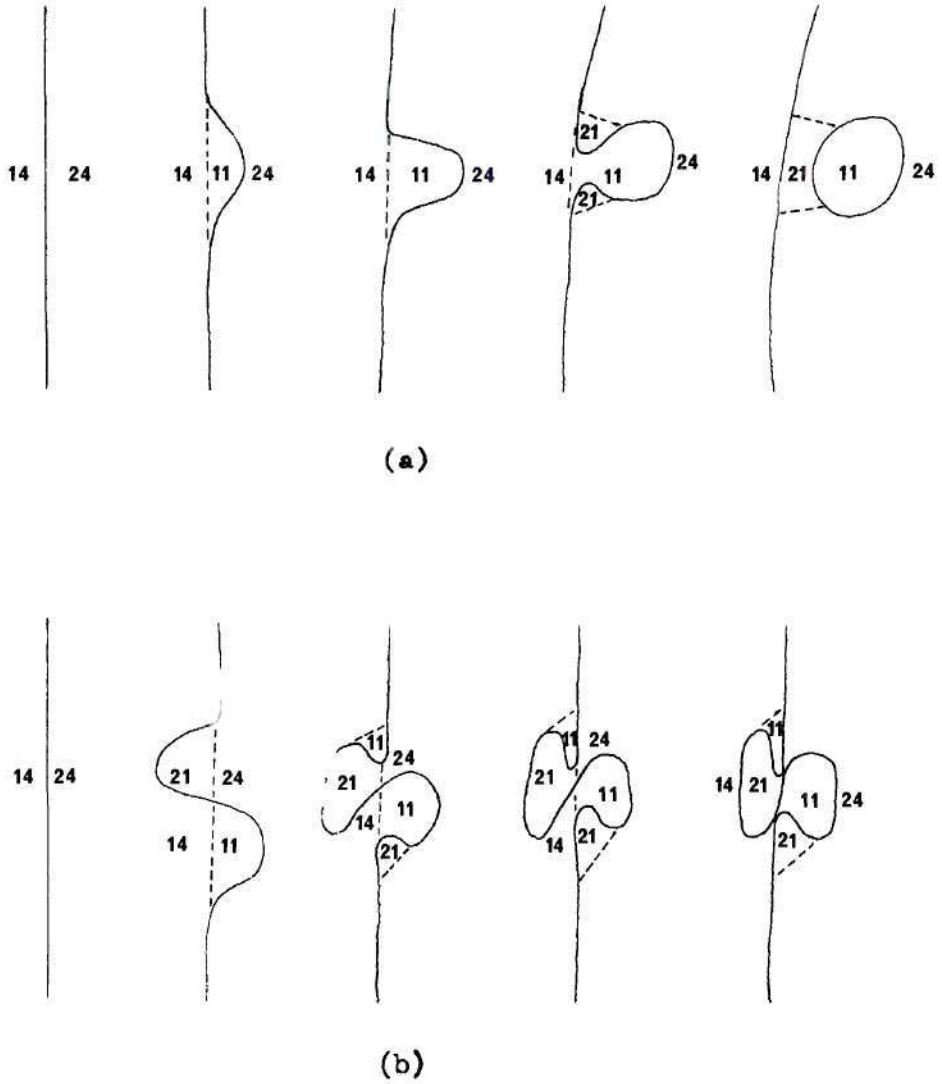

Figure 21. Strain-Induced Grain Boundary Migration. The Solid Lines Separate Grains while the Broken Lines Separate Mottled Structure from Structure with a Single Orientation Variant. The First Number Indicates the Grain and the Second Number Indicates the Number of Orientation Variants in the Region. (a). Showing the Creation of an Island. (b). Showing the Creation of Grain Boundary Component on Both Sides of Grain Boundary.

continuous physically and show similar microstructures both optically and in the TEM. The ease with which the component forms at the surface undoubtedly reflects the influence of constraint relaxations in selecting those variants which can grow. The work of Starke and Ling (23) has shown that domains which contract normal to the surface predominate in the late ordering stages in Ni_4Mo single crystals.

Evidence indicates that grain size affects the occurrence surface component. Paris (57) has observed no surface component in fine-grained samples of CuPt annealed at 500°C. Syutkin et al. (28, 32) have shown that cracking in CuAu annealed at low temperatures is seen only in coarse-grained samples. Apparently, the strains developed in corase-grained samples are greater than in fine-grained samples. Relaxation of constraints through growth of preferentially aligned domains coarse-grained samples develop the surface component.

The ordering transformation at 700°C appears to be more rapid than at 300°C or 500°C as would be expected. The evidence for this is the more rapid evolution of the microstructure and the accompanying hardness changes. At the high temperature, the mottled structure coarsens directly into a twinned structure of ordered variants which appear to form by thermally activated growth rather than stress relief twinning. The curving APB network observed within the matrix and within the larger twins at intermediate times would be expected from the growth and coalescence of domains of the same orientation which are out of phase. Since the boundaries between unlike adjacent variants show δ-fringe contrast indicative of interface strain, the progress of the coarsening process should be determined by the competition between the negative

volume ΔF of ordering, the positive interface ΔF of ordering (the mix-match at the interface is a function of the degree of order), the tendency to eliminate interfacial area, and the activation energy required to overcome metastable domain boundary networks. At 700°C this is accomplished without the formation and growth of the "recrystallized" component.

The contrast between a continuous ordering mechanism at high temperatures and a discontinuous mechanism at low temperatures appears in other polycrystalline neostructural systems such as CuAu (1), CoPt (24), Ni_2V (8), and Ni_4Mo (27). The formation of the grain boundary component in CuPt is clearly part of the transformation mechanism rather than just a mechanism of strain relief. The same conclusion may be valid for other neostructural systems although information regarding the degree of order within the different components is not available. Since lattice parameters are in general a function of temperature as well as a function of degree of order, it is possible that the ordering strains developed in the mottled structure are greater at low temperatures. At low temperatures the competing strain prevents the transformation from progressing to the fully ordered state without the domain coarsening provided by the migration of high angle grain boundaries. At high temperatures the lower strain and increased thermal activation permits the direct coarsening of the mottled structure.

The relationship between hardness and microstructure is too complex to explain in detail from the available information. However, four facts are apparent from the data obtained in this study. (i) Maximum hardness is obtained with a fine domain structure at intermediate degrees

of order as evidenced by the high hardness of the mottled structure. (ii) Coarse domained fully-ordered structures are relatively soft and may be softer than the as-quenched state (for instance, at 700°C). (iii) An important component of the hardening mechanism is the strain associated with order. (This conclusion is inferred from the fact that order strains are high enough to cause grain boundary cracking.) (iv) More than one hardening mechanism operates as indicated by the distinct two-stage hardening at 700°C.

Several mechanisms may be considered to contribute to the hardness of the mottled structure. Domain boundaries separating adjacent variants should impede the motion of dislocations since, as pointed out by Corke et al. (50), a dislocation on a given slip plane may be required to change from a unit dislocation to a superdislocation as it crosses the boundary. In addition, the misfit strain at the interface should provide some restraint. If the mottled structure contains order-disorder boundaries, the hardening may also be explained in terms of Fleischer's mechanism (36) as adopted by Cahn (1) or in terms of a similar mechanism adopted by Tanner (7).

The distribution of strains within a partially ordered structure of many domain boundaries is difficult to predict. For large domain sizes such as in the "recrystallized" regions, they are likely to be highly localized at the boundaries; however, for small domains, as in the mottled region, the grain boundary cracking indicates that long-range strains are present. In the case of Ni_4Mo (23), the root-mean-square strain has been shown to be directly related to the yield strength. Hence as the mottled structure develops and increases in degree of order

one would expect the rms strain to increase and, along with it, the hardness. As the mottled structure coarsens into twins (as at 700°C) the strain and hardness begin to drop. If the degree of order within the domains has not yet reached unity one would expect a second smaller peak in hardness to develop by means of the superdislocation model of Stoloff and Davies (19). At 300°C and 500°C peak hardness is evidently not reached in the mottled region and softening occurs with the appearance of the recrystallized component.

CHAPTER V

CONCLUSIONS AND RECOMMENDATIONS

Conclusions

1. A mottled structure, consisting of small domains of all four ordered variants and having a low degree of order, appears initially at all three annealing temperatures.
2. At 300 °C and 500°C coarsening is prevented by lattice strains severe enough to cause grain boundary cracking and as a result the mottled structure persists with little coarsening until consumed by a "recrystallized" component with a higher degree of order.
3. The "recrystallized" component consists of large highly ordered domains of one orientation variant and is formed by the mechanism of grain boundary migration.
4. At 700°C increased thermal activation and lower strains permit the domains of the mottled structure to coarsen directly into a twinned structure with twins lying on {100} and {011} type planes.
5. Hardness maxima correspond to the fine-domained mottled structure, and are followed by a decline in hardness associated with the appearance of coarse-domained structures: at high temperatures, the twinned structure, and at low temperatures, the "recrystallized" component.
6. A second hardness peak observed at 700 °C is attributed to high

hardness expected at intermediate degrees of order.

Recommendations for Further Study

A clear understanding of the order hardening in CuPt obviously requires more detailed and quantitative information regarding the transformation and deformation systems of this system. X-ray diffraction studies of the degree of order and rms strain developed over the range of temperatures would be of definite value. TEM studies of deformed samples would be useful in determining the operating slip systems (or twinning modes if such is the case), dislocation interactions with domain boundaries and so forth. For correlation with mechanical properties such information would be better interpreted in light of controlled tensile tests rather than simple hardness measurements.

The microstructure of the as-quenched samples and the mottled structure should be investigated by field ion microscopy since it offers some advantages over the TEM in high resolution studies. The exact nature of the mottled region could perhaps be determined.

It would also be interesting to quench several samples from above T_c to the itothermal annealing temperature in order to avoid rapid nucleation at low temperatures encountered in quenching to room temperature and reheating. It is expected that the microstructure at the high temperatures would develop much differently.

APPENDICES

APPENDIX I

INDEXING OF SELECTED AREA DIFFRACTION PATTERNS IN CUPT

During ordering, the unit cell of CuPt changes from cubic face centered to rhombohedral with a rhombohedral angle of about 91°. Since the ordered lattice is nearly cubic, a cubic unit cell can be imagined whose axes are twice as long as those of the conventional fcc cell. Thus, the new unit cell is made up of eight of the original fcc cells and contains 32 atoms. It is convenient to refer indices of reflections occurring in the ordered structure to this particular cell. Note that the usual indices of fundamental fcc reflections are doubled.

In calculating the structure factors for ordered CuPt, Johansson and Linde (39) use a rhombohedral cell which contains 8 atoms. The relation of this unit cell to the unit cell of the cubic superlattice is shown in the model pictured in Figure 22. Copper atoms are located at 000, $\frac{1}{2}\frac{1}{2}0$, $\frac{1}{2}0\frac{1}{2}$ and $0\frac{1}{2}\frac{1}{2}$, while platinum atoms are located at $\frac{1}{2}00$, $0\frac{1}{2}0$, $00\frac{1}{2}$ and $\frac{1}{2}\frac{1}{2}\frac{1}{2}$. Referred to the rhombohedral cell the structure factors of CuPt are:

$$F_{hkl} = 0, \tag{1}$$

when h, k, and l are mixed (both odd and even);

$$F_{hkl} = 4\ (f_{cu} + f_{pt}) \tag{2}$$

when h, k, and l are all even and

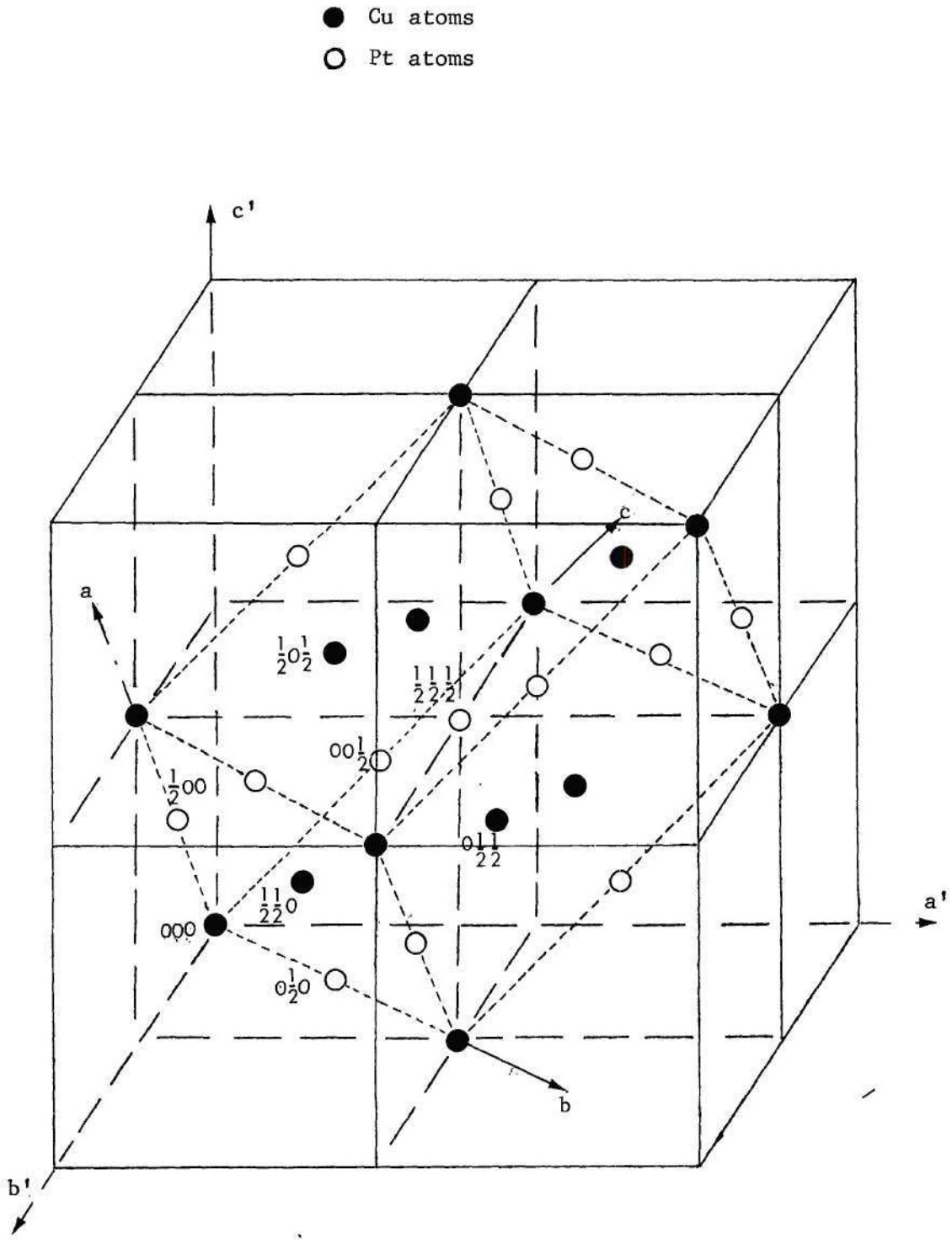

Figure 22. Model of CuPt Superlattice with Eight-Atom Rhombohedral Unit Cell Outlined Inside.

$$F_{hkl} = 4\ (f_{cu} - f_{pt}) \qquad (3)$$

when h, k, and l are all odd. The rhombohedral indices h, k, and l can be obtained from the cubic superlattice indices h', k', and l' by the transformations

$$h = (k' + l')/2, \qquad (4)$$

$$k = (h' + k')/2, \qquad (5)$$

and

$$l = (h' + l')/2, \qquad (6)$$

where it is assumed that the layering is on the (222) plane of the cubic superlattice. (From here forward, all indices in the Appendices refer to the cubic superlattice unless noted.) Using these transformations, Table 1 shows the classification of each low index spot in the cubic superlattice. In the table "Fundamental" reflections have structure factors given by Equation (2) and are the same reflections produced by the disordered lattice except that the indices have been doubled. "Superlattice" reflections have structure factors given in Equation (3) and are the "extra" reflections due to layering on the (222) plane. The reflections that have the structure factor of Equation (1) have no intensity and are hence "extinct". Reflections which have mixed indices in the cubic will also have mixed indices in the rhombohedral coordinates and hence are not tested in Table 1.

It is clear that only odd values of h', k', l' correspond to possible superlattice reflections and only even values correspond to possible

Table 1. Classification of Reflections for Layering on (111) Plane of Cubic Ordered Cell.

Indices of Reflections Referred to Cubic Superlattice, h'k'l'	Indices of Reflections Referred to Rhombohedral Unit Cell, hkl	Type of Reflection
111	111	Superlattice
$11\bar{1}$	010	Extinct
$1\bar{1}\bar{1}$	$00\bar{1}$	"
$1\bar{1}1$	100	"
200	110	"
020	011	"
002	101	"
220	121	"
202	211	"
022	112	"
$\bar{2}20$	$\bar{1}01$	"
$\bar{2}0\bar{2}$	$0\bar{1}1$	"
$02\bar{2}$	$\bar{1}10$	"
311	221	"
131	122	"
113	212	"
$\bar{3}11$	$\bar{1}\bar{1}1$	Superlattice
$3\bar{1}1$	210	Extinct
$31\bar{1}$	120	"
$\bar{1}31$	012	"
$1\bar{3}1$	$1\bar{1}\bar{1}$	Superlattice
$13\bar{1}$	021	Extinct
$\bar{1}13$	102	"
$1\bar{1}3$	201	"
$11\bar{3}$	$\bar{1}1\bar{1}$	Superlattice
222	222	Fundamental
$22\bar{2}$	020	"
$2\bar{2}\bar{2}$	$00\bar{2}$	"
$2\bar{2}2$	200	"
400	220	"
040	022	"
004	202	"
$33\bar{1}$	131	Superlattice
$3\bar{1}3$	311	"
$\bar{1}33$	113	"
(no contrast for remaining nine permutations of (331)		

fundamental reflections. Furthermore only certain combinations of h'k'l' give non-zero structure factors. The superlattice reflections that appear depend on which particular variant is present (i.e. the plane on which layering occurs) as discussed in the preceeding paragraph. For even indices, the set of numbers obtained on dividing by two is either mixed or unmixed. For the former case the structure factor is zero and for the latter it is given by Equation 2.

Tables similar to Table 1 can be made for ordering on other {222} planes. To do this, transformation Equations (4), (5) and (6) are changed so that the rhombohedral cell is oriented properly with respect to the new ordering. The resulting classification of reflections is almost exactly that of Table 1. The only reflections which undergo a change are those whose cubic indices are all odd. In Table 1, indices which are all odd are classified either as extinct or as being superlattice spots. For instance, of the four {111} positions, one is superlattice and three have no intensity. Of the twelve {311} positions, three are superlattice and nine have no intensity. In general for indices which are all odd and the same distance from the origin in reciprocal space, one-fourth of the positions have superlattice spots and the remaining positions have no intensity. When the ordering is some other {222} plane one-fourth of the spots are still superlattice but for each {222} plane it is a different one-fourth. Thus every position whose indices are all odd in the cubic reciprocal lattice shows a superlattice spot for ordering on <u>one</u> of the possible {222} planes. In this study the four ways the {222} ordering can form have been called "orientation variants" (see Figure 23). Table 2 lists the indices which are superlattice spots for each of

the orientation variants.

If the (111) and ($\bar{1}\bar{1}1$) superlattice spots appear in a selected area diffraction pattern, one is sure that orientation variants type 1 and type 2 (Figure 23) are present in the region. However, one is not able to say anything about orientation variants types 3 and 4. By constructing a reciprocal lattice model which contained superlattice spots for all four orientation variants of CuPt, it is seen that no plane in reciprocal space could contain superlattice spots from more than two orientation variants. Figures 24 and 25 show diffraction patterns of the (111) and (112) planes in reciprocal space when zero, one, and two orientation variants are responsible for the superlattice spots. These two planes are the most commonly viewed planes which contain superlattice spots. It will be noted that several of these diffraction patterns are easily confused.

The reciprocal lattice model is also useful in interpreting Figure 26a. The same arrangement of hexagons as in Figure 26a is found when one looks down the [111] body diagonal of the reciprocal lattice model as is shown in Figure 26b. With further examination of the reciprocal lattice model, all the spots in Figure 26a can be identified. Figure 26a turns out to be a plane near the zeroth order reciprocal lattice plane. It is tilted off this plane such that spots from the Laue zones (59) above and below the zeroth order Laue zone have become visible. Since more than a single plane in reciprocal space is included in this image, superlattice spots from more than two orientation variants can contribute to the diffraction pattern. This has occurred; in Figure 26a there are superlattice spots corresponding to all four orientation variants.

Table 2. Summary of Superlattice Reflections in CuPt

Orientation Variant (222)	Orientation Variant ($22\bar{2}$)	Orientation Variant ($2\bar{2}2$)	Orientation Variant ($\bar{2}22$)
111	$11\bar{1}$	$1\bar{1}1$	$\bar{1}11$
$\bar{3}11$	$3\bar{1}1$	$31\bar{1}$	311
$1\bar{3}1$	$\bar{1}31$	131	$13\bar{1}$
$11\bar{3}$	113	$\bar{1}13$	$1\bar{1}3$
$33\bar{1}$	331	$\bar{3}31$	$3\bar{3}1$
$3\bar{1}3$	$\bar{3}13$	313	$31\bar{3}$
$\bar{1}33$	$1\bar{3}3$	$13\bar{3}$	133
511	$51\bar{1}$	$5\bar{1}1$	$\bar{5}11$
151	$15\bar{1}$	$1\bar{5}1$	$\bar{1}51$
115	$11\bar{5}$	$1\bar{1}5$	$\bar{1}15$
333	$33\bar{3}$	$3\bar{3}3$	$\bar{3}33$
$5\bar{3}1$	$\bar{5}31$	531	$53\bar{1}$
$\bar{3}51$	$3\bar{5}1$	$35\bar{1}$	351
$51\bar{3}$	513	$\bar{5}13$	$5\bar{1}3$
$\bar{3}15$	$3\bar{1}5$	$31\bar{5}$	315
$15\bar{3}$	153	$\bar{1}53$	$1\bar{5}3$
$1\bar{3}5$	$\bar{1}35$	135	$13\bar{5}$

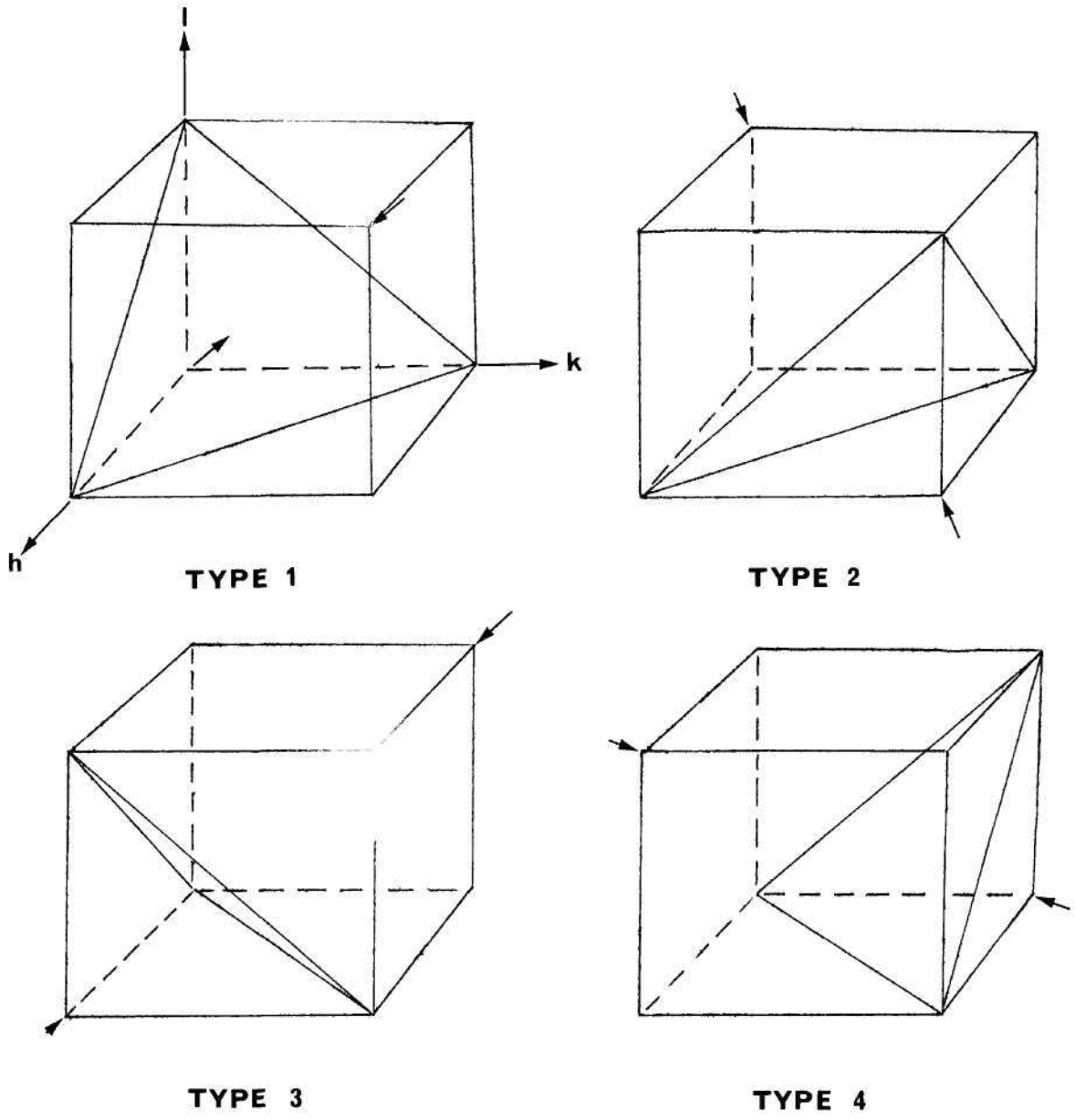

Figure 23. Orientation Variants of CuPt.

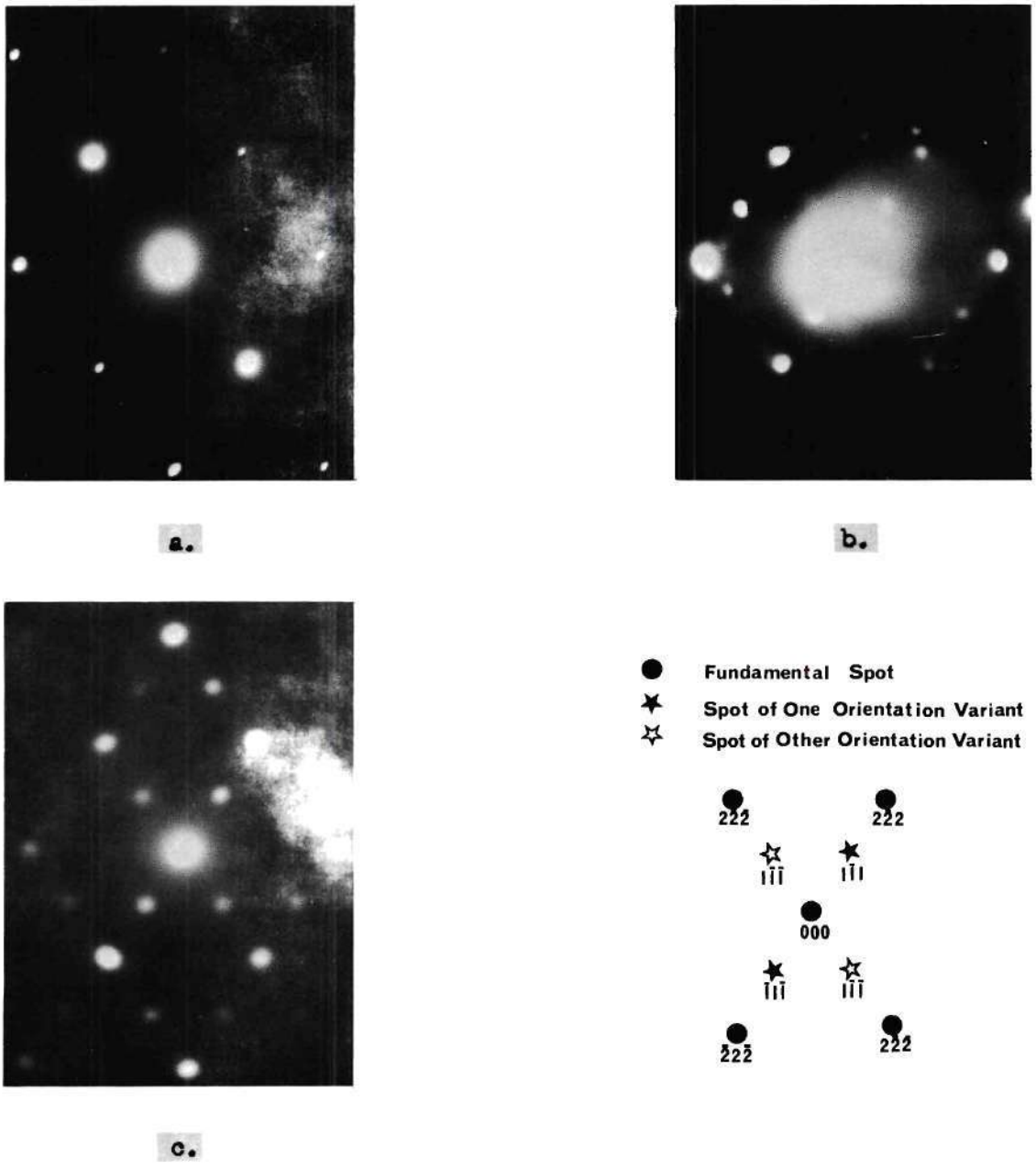

Figure 24. Diffraction Patterns of CuPt in (110) Orientation. a. Showing no Superlattice Spots. b. Showing Superlattice Spots of One Orientation Variant. c. Showing Superlattice Spots of Two Orientation Variants. d. Diagram Showing Indices of Spots in (110) Patterns.

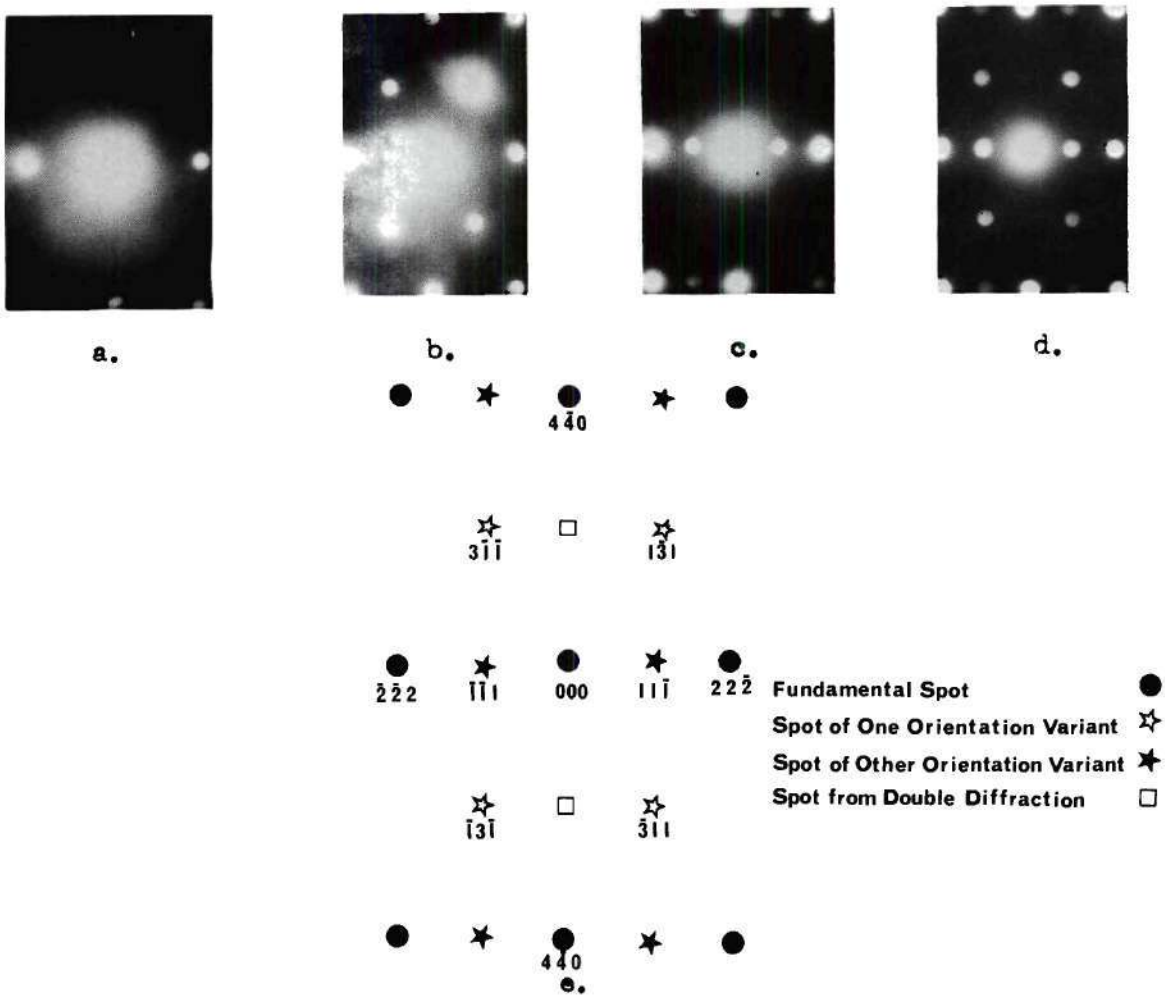

Figure 25. Diffraction Patterns of CuPt in (112) Orientation. a. Showing No Superlattice Spots. b. Showing Superlattice Spots of One Orientation Variant. c. Showing Superlattice Spots of One Orientation Variant. d. Showing Superlattice Spots of Two Orientation Variants. e. Diagram Showing Indices of Spots in (112) Pattern.

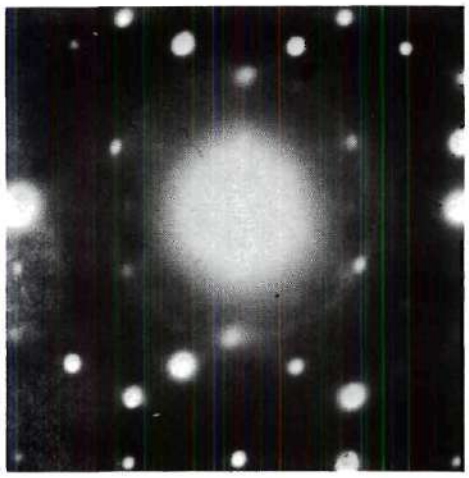

a.

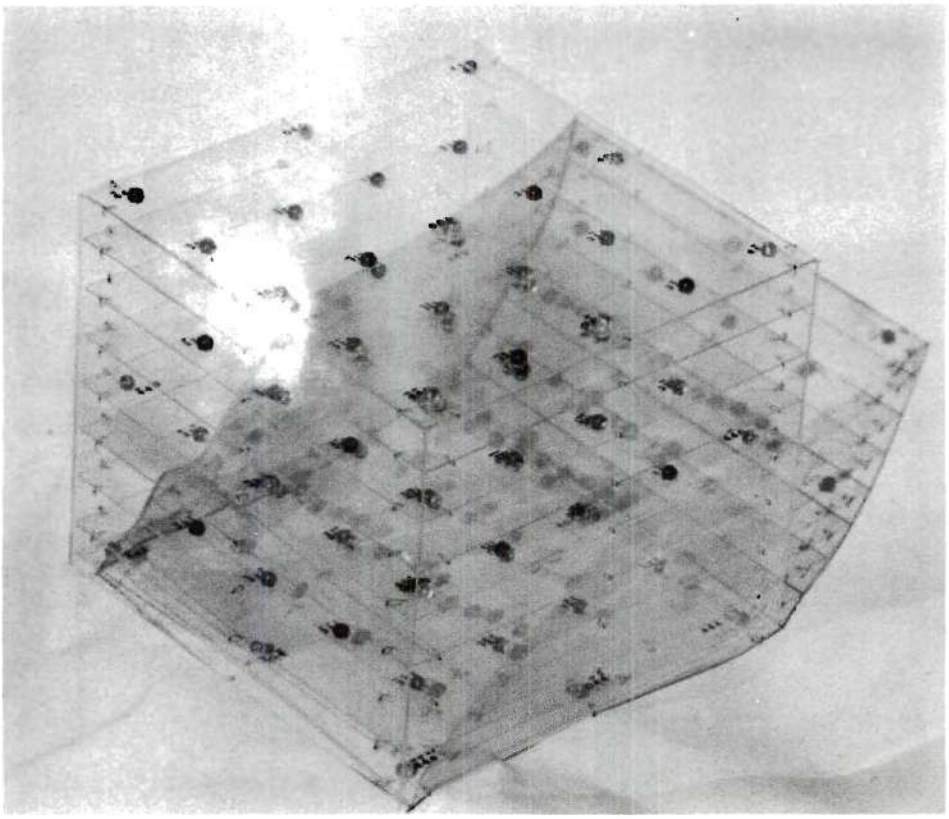

b.

Figure 26. Multiple Laue Zones in Diffraction Patterns of CuPt. a. Diffraction Pattern Showing (111) Orientation and Spots from First-Order Laue Zones. b. Reciprocal Lattice Model of CuPt Viewed Down [111] Axis.

APPENDIX II

COHERENT TWIN PLANES IN CUPT

It has been found that twins developing in CuPt have {100} or {110} habit planes. Some of the previous analysis in the text has been based on the assumption that the habit plane and coherent twin plane are one in the same. It is the purpose of this section to designate in table form the possible twin planes separating the different orientation variants.

The orientation variants are labeled according to the scheme adopted in Figure 23: type 1 corresponds to ordering on (111), type 2 to ordering on $(\bar{1}\bar{1}\bar{1})$, type 3 to ordering on $(\bar{1}11)$, type 4 corresponds to ordering on $(1\bar{1}1)$. The coherent twin plane for any pair of variants is a mirror plane of symmetry. For any given pair there are two possible planes as shown in Table 3. The atomic movements to generate the twins have not been considered.

Table 3. Coherent Twin Planes of CuPt

Orientation Variant Type	+ Orientation Variant Type	Forms Coherent or ( )	Interfaces On ( )
1	2	(110)	(001)
1	3	(011)	(100)
1	4	(101)	(010)
2	3	$(10\bar{1})$	(010)
2	4	$(01\bar{1})$	(100)
3	4	$(1\bar{1}0)$	(001)

LITERATURE CITED

1. V. S. Arunachalam and R. W. Cahn, Journal of Materials Science 2 (1967) 160-170.

2. B. Chakravarti, E. A. Starke and B. G. LeFevre, "Order-Induced Strengthening in Ni_4Mo," Journal of Materials Science 5 (1970) 394-406.

3. W. L. Bragg and E. J. Williams, Proceedings of the Royal Society A145 (1934) 699 and A151 (1935) 540.

4. L. Guttman, "Order-Disorder Phenomena in Metals," Solid State Physics 3 (Academic Press, New York, 1956) 145.

5. J. W. Christian, The Theory of Transformations in Metals and Alloys (Pergamon Press, New York, 1965) 697.

6. J. S. Bowles and A. S. Malin, "Phase Transformations Accompanying the Formation of A. B. Superlattices," Journal of the Australian Institute of Metals 5 (1966) 131.

7. L. E. Tanner, Physica Status Solidi 30 (1968) 685.

8. L. E. Tanner, "The Ordering of Ni_2V -- Initial Observations," Ordered Alloys--Structural Applications and Physical Metallurgy presented at the Third Bolton Landing Conference, Lake George, New York, September 8-10, 1969 (Baton Rouge, Claitor's Publishing Division, 1970) 253.

9. H. N. Southworth and B. Ralph, "The Mechanism of Formation of the Li_o Superlattice," Conference on Mechanisms of Phase Transformations in Crystalline Solids (Institute of Metals Monograph No. 33, Manchester, 1969) 224.

10. B. G. LeFevre and R. W. Newman, "The Study of Ordered Alloys by Field-Ion Microscopy," Applications of FIM in Physical Metallurgy and Corrosion (Georgia Institute of Technology, Atlanta, Georgia, December 1969) 243.

11. R. W. Cahn and R. S. Irani, "A Classical Phase Transformation: Order-Disorder in CuPt," Nature 226 (June 13, 1970) 1045.

12. P. S. Rudman, "Order-Disorder and Radiation Damage," Intermetallic Compounds (Wiley, New York, 1967).

13. M. Hillert, Acta Metallurgica 9 (1961) 525.

14. H. E. Cook, D. de Fontaine and J. E. Hilliard, "A Model for Diffusion on Cubic Lattices and Its Application to the Early Stages of Ordering," Acta Metallurgica 17 (1969) 765.

15. Fu-Wen Ling and E. A. Starke, "The Kinetics of Disorder-Order Transformations," Scripta Metallurgica 5 (1971) 741-748.

16. A. G. Guy, Elements of Physical Metallurgy (Addison Wesley, Reading, Massachusetts, 1967) 460.

17. M. Hirabayashi and S. Weissman, "Study of CuAuI by Transmission Electron Microscopy," Acta Metallurgica 10 (January 1962) 25.

18. B. G. LeFevre, "Field-Ion Studies of Microstructures and Transformations in Long-Range Ordered Alloys," Surface Science 23 (1970) 144-159.

19. N. S. Stoloff and R. G. Davies, "The Mechanical Properties of Ordered Alloys," Progress in Materials Science 13, No. 1 (Pergamon Press, Oxford, 1966) 3-84.

20. R. W. Cahn, "Correlation of Local Order with Mechanical Properties," Local Atomic Arrangements Studied by X-ray Diffraction, ed. by J. B. Cohen and J. E. Hilliard (Gordon and Breach, New York, 1966) 179.

21. J. B. Cohen, "A Brief Review of the Properties of Ordered Alloys," Journal of Materials Science 4 (1969) 1012-1022.

22. S. L. Mannan and V. S. Arunachalam, "Low Temperature Ordering in CuAu," Scripta Metallurgica 3 (1969) 597-600.

23. Fu-Wen Ling and E. A. Starke, "The Development of Long-Range Order and the Resulting Strengthening Effects in Ni_4Mo," Acta Metallurgica 19 (August 1971) 759.

24. J. B. Newkirk, A. H. Geisler, D. L. Martin, and R. Smoluchowski, "Ordering Reaction in Cobalt Platinum Alloys," Transactions AIME 188 (October 1950) 1249.

25. J. B. Newkirk, R. Smoluchowski, A. H. Geisler, and D. L. Martin, "Phase Equilibria in an Ordering Alloy System," Journal of Applied Physics 22, No. 3 (March 1951) 290.

26. J. B. Newkirk, R. Smoluchowski, A. H. Geisler, and D. L. Martin "Diffuse Scattering by an Ordering Alloy," Acta Crystallographica 4 (1951) 507.

27. W. B. Snyder and C. R. Brooks, "Mechanical Properties and Domain Structure of Ordered Ni_4Mo," Ordered Alloys--Structural Applications and Physical Metallurgy presented at the Third Bolton Landing Conference, Lake George, New York, September 8-10, 1969 (Claitor's Publishing Division, Baton Rouge, 1970) 275.

28. P. N. Syutkin, V. I. Syutkina, O. D. Shashkov, E. S. Yakovleva, and N. N. Buinov, "Two Mechanisms of Domain Structure Formation in CuAu on Ordering," Ordered Alloys--Structural Applications and Physical Metallurgy presented at the Third Bolton Landing Conference, Lake George, New York, September 8-10, 1969 (Claitor's Publishing Division, Baton Rouge, 1970) 227.

29. R. Gevers, J. Van Landuyt, and S. Amelinckx, "Intensity Profiles for Fringe Patterns Due to Planar Interfaces as Observed by Electron Microscopy," Physica Status Solida 11 (1965) 689.

30. L. E. Tanner and M. F. Ashby, "On the Relief of Ordering Strains by Twinning," Physica Status Solids 33 (1969) 59.

31. B. Hansson and R. S. Barnes "On Order Twinning in AuCu," Acta Metallurgica 12 (1964) 315.

32. P. N. Syutkin, V. I. Syutkina, E. S. Yakovleva, "Spontaneous Cracking of the Alloy CuAu on Ordering," Physics of Metals and Metallography 27, No. 5, (1969) 142-147.

33. B. A. Grinberg, V. I. Syutkina, and E. S. Yakovleva, Physics of Metals and Metallography 26, No. 1 (1968) 17-25.

34. D. W. Pashley, J. L. Robertson, and M. J. Stowell, Philosophical Magazine 19 (1969) 83.

35. R. W. Cahn, Physical Metallurgy ed. by R. W. Cahn (North Holland Publishing Company, Amsterdam, 1965) 958.

36. R. L. Fleischer, "Effects of Non-Uniformities on the Hardening of Crystals," Acta Metallurgica 8 (1960) 598.

37. M. Hansen and K. Anderko, Constitution of Binary Alloys (McGraw-Hill Book Company, New York, 1958) 617.

38. W. B. Pearson, Lattice Spacings and Structures of Metals and Alloys (Pergamon Press, London, 1958) 174, 229, 597.

39. C. H. Johansson and J. O. Linde, Annalen der Physik 82 (1927) 459-477.

40. N. S. Kurnakow and W. A. Nemilow, Zeitschrift fur Anorganische und Allgemeine Chemie 210 (1933) 1-12.

41. J. O. Linde, Annalen der Physik 30 (1937) 151-164.

42. A. Schneider and U. Esch, Z. Elektrochem. 50 (1944) 290-301.

43. C. B. Walker, "X-ray Measurements of Order in CuPt," Journal of Applied Physics 23, No. 1 (1952) 118.

44. P. Assayag and M. Dode, Comptes rendus Academie des Sciences (Paris) 239 (1954) 762.

45. R. S. Irani and R. W. Cahn, "A Thermal Polishing Technique for Use with Polarized Light," Metallography 4 (1971) 91-93.

46. J. C. Slater, "Note on Superlattices and Brillouin Zones," Physical Review 84, No. 2 (October 15, 1951) 179.

47. J. F. Nicholas, "Effect of the Fermi Energy on the Stability of Superlattices," Proceedings of the Physical Society (London) A66 (1953) 201.

48. Barton Roessler and John A. Rayne, Physical Review 136, No. 5A (November 30, 1964) A1380.

49. L. Nowack, Zeitschrift fur Metallkunde 22 (1930) 94-103.

50. N. T. Corke, S. Amelinckx, and J. Van Landuyt, Materials Research Bulletin 4 (1969) 289-296.

51. C. T. J. Ahlers and R. W. Balluffi, Journal of Applied Physics 38 (1967) 91P.

52. O. G. Brooks, A Field Ion Microscope Study of the Ordering Alloys Cu_3Pt and CuPt, (Master's Thesis, Vanderbilt University, 1971).

53. P. B. Hirsch, A. Howie, R. B. Nicholson, D. W. Pashley, and M. J. Whelan, Electron Microscopy of Thin Crystals (Butterworths, London, 1965).

54. C. K. H. DuBose and J. O. Stiegler, "Semiautomatic Preparation of Specimens for Transmission Electron Microscopy," ORNL-4066 (February 1967).

55. M. A. P. Dewey and T. G. Lewis, Journal of Scientific Instruments 40 (1963) 385.

56. L. E. Murr, Electron Optical Applications in Materials Science (McGraw-Hill Book Company, New York, 1970).

57. H. Paris, private communication.

58. P. B. Hirsch, et al., op. cit., 117.

59. Ibid., 112.

60. V. S. Arunachalam and R. W. Cahn, "Stress-Ordering of CuAu," Ordered Alloys--Structural Applications and Physical Metallurgy presented at the Third Bolton Landing Conference, Lake George, New York, September 8-10, 1969 (Claitor's Publishing Division, Baton Rouge, 1970) 215.